DEPARTMENT OF PHYSICS
UNIVERSITY OF JYVÄSKYLÄ

ELECTRONIC STRUCTURE OF TRIANGULAR, HEXAGONAL AND ROUND GRAPHENE FLAKES

BY
HEIKKI HEISKANEN

Thesis for the Degree of
Licentiate of Philosophy

JYVÄSKYLÄ, FINLAND
MARCH 2009

Preface

This research was carried out during the years 2006-2008 at the University of Jyväskylä, Department of Physics and finished in 2009. I would like to express my gratitude to Professor Matti Manninen whose supervision and guidance was essential for this thesis to come true. A special thanks goes also to Dr. Jaakko Akola for all his help in this research. Last but not least I would like to thank my dearest Virve for all her love and support.

In Jyväskylä, 7 March 2009

Heikki Heiskanen

Heiskanen Heikki
Electronic Structure of Triangular, Hexagonal and Round Graphene Flakes
University of Jyväskylä; 2009
(Theoretical study / Department of Physics, University of Jyväskylä)
Licentiate Thesis

Supervisor:
Professor Matti Manninen, University of Jyväskylä, Finland

Reviewers:
Jouko Nieminen, Tampere University of Technology, Finland
Kalevi Kokko, University of Turku, Finland

Abstract

The electronic shell structures of triangular, hexagonal and round graphene quantum dots (flakes) were studied using mainly a simple tight-binding method (TB). Density functional calculations demonstrated that the electronic structure near Fermi energy and at the bottom of the band is correctly described with this simple TB, where only the p_z -orbitals perpendicular to the graphene plane are included. The results show that for triangular flakes at the bottom and at the top of the p_z band a super shell structure, similar to that of free electrons confined in a triangular cavity, is seen and near the Fermi level, the shell structure is that of free *massless* particles. Also close to E_f triangles with armchair edges have an additional set of levels ("ghost states") absent for the zigzag edged flakes studied, while the latter exhibit prominent edge states at E_f. These "ghost states" are a result of the graphene band structure and the plane wave solution of the wave equation and so triangles with armchair edge can be used as building blocks to produce other types of flakes that also support these ghost states. Edge roughness has only a small effect on the band structure of the triangular flakes but quite significant effect on all the other types of flakes studied. In round flakes the states close to the Fermi energy are strongly dependent on the flake radius, and are always localized on the zigzag parts of the edge.

Contents

1 Introduction

Electronic transport through small quantum dots is dominated by the existence of discrete electron levels which cause conductance peaks whenever the level coincides with the Fermi level of the leads connected to the dot. If the quantum dot has a high symmetry, the levels will bunch in electron shells like in atoms. In the case of semiconductor quantum dot the shell structure has been observed in circular dots [1]. However, it is known that in two-dimensional systems also other geometries, especially the equilateral triangles [2], show clear shell structure. Moreover, in a triangle the modulation between the shells show as a persistent supershell structure [2].

Graphene offers a unique opportunity to make triangular and hexagonal quantum dots and to study their electronic structure. The main purpose of this research was to study the possibility of observing the supershell structure in triangular graphene quantum dots in the region where the electron have properties of massless particles. For comparisons also hexagonal and circular quantum dots were studied.

This thesis consists of three separate publications concerning the electronic properties of graphene and a short introductional part, in which some basics about the used research method and graphene itself as a material are introduced as well as a short summary of the results is given.

The first report [A] (appendix A) is a shorter letter type of publication, where only triangular graphene flakes are studied. In this letter also the accuracy of the simple tight-binding method with only one electron per atom was compared to the widely used density functional theory where all valence electrons are included. The results showed that indeed the simple tight-binding model describes correctly the electronic structure close to the Fermi level. This shorter study was published in *Physical Review B (2008)*.

The second report [B] (appendix B) was published in *New Journal of Physics* (2008) and is a wider study about different types of graphene flakes concentrating on the "near Fermi energy" area of the energy distribution. This research also goes deeper into studying the specific electronic shell structures and compares them between the different types of flakes: triangular, hexagonal and round.

The third paper [C] (appendix C) is a conference report which deepens the understanding of the supershell structure of graphene triangles and studies also quantum dots made with external potential in a large graphene sheet.

Next a brief presentation about the research subject –graphene, is given. Following that, the used research method –tight-binding (TB) is introduced and a short summary of the results is given. The heart of this thesis: the actual research and the results in detail are at the end as appendices (reports) A, B and C.

2 About Graphene

Graphite is an allotropic form of common coal. It consists of layers that are confined to each other very loosely (Figure 1a). In these layers the atoms are organized in a hexagonal "honey comp" pattern and a separate this kind of layer is called *graphene* (Figure 1b). Also carbon nanotubes, which are nowadays widely under investigation, can be considered to be graphene wrapped to a roll, as well as fullerines, that are ball-shaped graphene with pentagons in addition to hexagons in their lattice structure. Graphene is also famous for its extreme strength of tension.

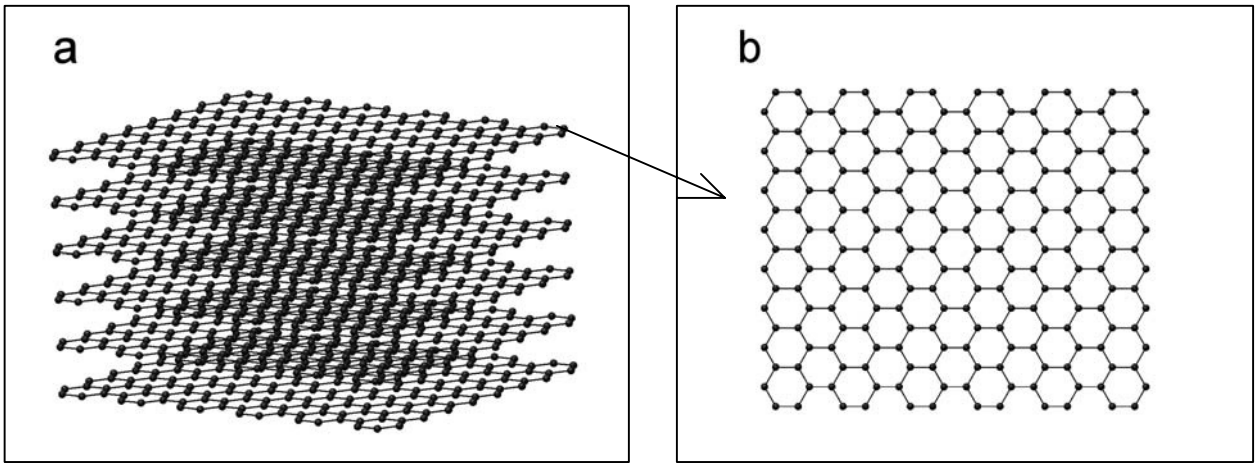

Figure 1: The structure of graphite (a) and the lattice structure of a single graphene sheet (b).

The thing that has made graphene so interesting is the recent experimental success in manufacturing it [3]-[6]. Particularly interesting is the band structure near Fermi energy: electrons and holes behave like massless particles (Dirac fermions) although their velocity is quite slow. This is a result of the linear dispersion relation [7]. Graphene, being just a single atomic layer, is in a sense two dimensional infinite confining potential for electrons. Due to this, flakes made of it are intriguing two dimensional quantum dots, which have even further peculiar features because of the honey comp structure. The two dimensional, one-layer essence of graphene gives fascinating starting point for theoretical researchers: Because of this one-layer property and the lattice structure, the sp^2 hybridized bonds of graphene leave in a sense one electron (bond) per atom free. These p_z electrons, perpendicular to the graphene plain are known to be the reason for the captivating band structure where the valence and the conduction bands meet at the corners of the hexagonal Brillouin zone (Figure 2) [8] [9]. Now, this basis allows different theoretical approaches, such as the tight-binding, to be applied in researches.

To understand the band structure it is worth mentioning that the Fermi surface consists of discrete set of these corner points of the hexagonal Brillouin zone (points of high k-value). Due to this, the density of states (DOS) has a zero weight (and zero band gap) at the Fermi energy (E_f). Every one of the crossover regions has an hourglass-like shape and this leads to the linear, isotropic dispersion relation in the conduction band, but only in a small energy region close to E_f.

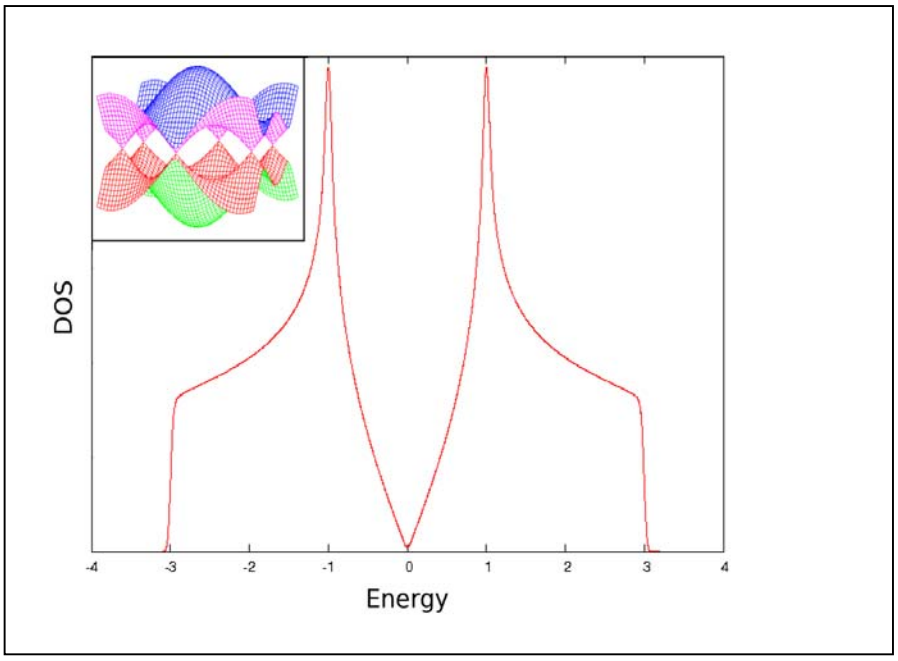

Figure 2: The tight-binding density of states (for p_z electrons) of an infinite graphene sheet (in arbitrary units). Inset: Tight-binding band structure of graphene showing the points at where the valence and conduction bands meet at the Brillouin zone boundary.

Due to its structure, there are two quite stable directions, graphene can be cut into: "zigzag" (zz) and "armchair" (ac) (Figure 3). This feature enhances the interest since, as shall be shown later in the results, the type of the edge quite largely determines the electronic properties of the graphene flakes. In addition to this, the triangular and hexagonal shapes can be cut from infinite graphene sheet exactly along these directions. Already in nanoribbons made of graphene, the cutting direction has been shown to play a crucial role in their physical properties [10] [11].

These properties of graphene, in addition to the shape effects of the flakes cut out of it, set an intriguing ground for this research to be carried out.

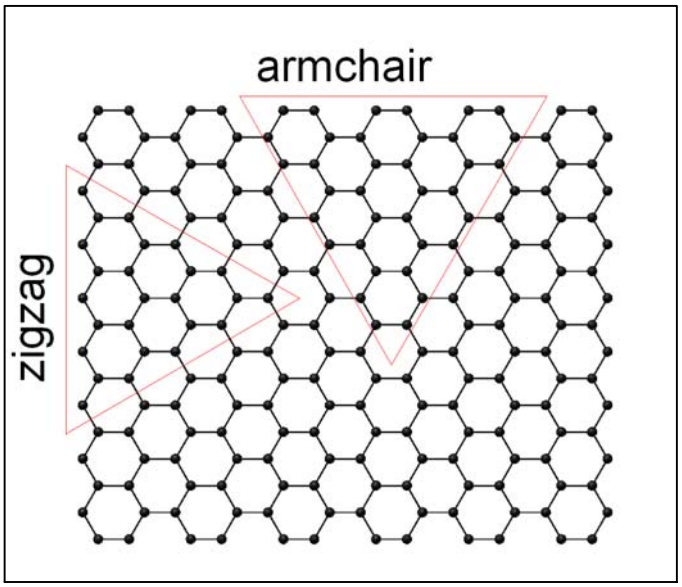

Figure 3: The two stable cutting directions of equilateral triangles of graphene: armchair (ac) and zigzag (zz).

3 Tight-Binding (*Hückel* Model)

Tight-binding (TB), in a nut shell, is a simplified method for defining quantum mechanical variables. It can be applied in cases where the free electron model does not work and the electrons can be considered to be mainly confined (localized) to the atomic sites. The starting point for TB model is a single isolated atom, for which the electronic states are discrete energy levels. After this a solid or a lattice is considered to be formed by bringing together a large number of these atoms. The atomic states will then split due to the interactions between atoms and because of the amount of the atoms this leads to a quasi-continuous band of states. The closer to each other the atoms are forced the grater the interactions become and hence the wider the bands get. Thus these bands can also result from the overlap and interactions of the atomic orbitals including the possibility of free-electron-like behaviour. About this and tight-binding in general (infinite case) can be read for example in [8].

In the case under study, how ever, there is only a finite lattice with N atoms in it. Also the interest is mainly in the wave functions of the lattice level rather than in the level of atomic wave functions. So as a starting point it is assumed that the electron wave function Φ_j for the *j*th atom is known and the total wave function Ψ is taken as the linear combination of all these atomic states Φ_j, which are so being considered to be the basis vectors:

$$\Psi = \sum_{j=1}^{N} c_j \Phi_j \tag{1}$$

Now the basic Schrödinger equation gives:

$$H\Psi = E\Psi \tag{2}$$

leading to the following:

$$\sum_{j=1}^{N} H c_j \Phi_j = \sum_{j=1}^{N} E c_j \Phi_j \tag{3}$$

If this is now multiplied from left by Φ_i and integrated, it becomes:

$$\sum_{j=1}^{N} c_j \int \Phi_i^* H \Phi_j \, dv = \sum_{j=1}^{N} c_j E \int \Phi_i^* \Phi_j \, dv$$

giving the simplified form:

$$\sum_{j=1}^{N} c_j (H_{ij} - E S_{ij}) = 0 \tag{4}$$

that applies for all *i* and where:

$$H_{ij} = \int \Phi_i^* H \Phi_j \, dv \qquad \text{and} \tag{5a}$$

$$S_{ij} = \int \Phi_i^* \Phi_j \, dv \tag{5b}$$

This simple model above is called the *Hückel* model.

Now, since in graphene the relevant p_z electrons are perpendicular to the graphene plain, their interactions with the neighbouring atoms are directionally independent and consequently they can be considered as s-type electrons (in the atomic Φ_i level). It can also be assumed that:

- the overlap between atomic sites can be neglected: $S_{ij} = 0$, when $i \neq j$
- only the nearest neighbour interactions are relevant: $H_{ij} \neq 0$ only if i and j are nearest neighbours or $i = j$
- the on-site energy can be set to zero: $H_{ii} = 0$.

This way the problem culminates to a very basic matrix form, where the Hamiltonian matrix of the system becomes (6):

$$H_{ij} = \begin{cases} -t & \text{if } i \text{ and } j \text{ are nearest neighbours} \\ 0 & \text{otherwise} \end{cases} \quad (6)$$

Here the hopping parameter t determines the width of the bands and, as mentioned, the on-site energy is set to be zero ($E_f = 0$). In the calculations the units are chosen to be according to $t = 1$. Because of this the TB bands will reach from -3 to +3 (as it is in Figure 2). In reality for graphene the actual t corresponds to about t = 2,6eV.

In real life cutting finite flakes from infinite graphene sheets breaks the covalent bonds and leads to dangling bonds at the edges of the flakes. These edges then have to be passivated for example with hydrogen. This kind of a passivation, how ever, has only a small effect on the p_z electronic states, since also the covalent bonding with hydrogen involves sp^2 hybridized orbitals. For that reason the effects of the dangling bonds can be neglected and treat the edge atoms in the same way as bulk atoms following Areshkin et al [9]. In addition to this, the interactions with possible substrate will also be neglected and the graphene flakes will be treated as isolated two dimensional quantum dots.

In this research, all the eigen values of the Hamiltonian matrix problem above ((4) - (6)) are relevant, since the interest of this research is both at the bottom and at the middle (Fermi energy) of the energy distribution. In the calculations the amount of atoms in the triangular flakes ranged from about 5 000 to about 44 000, making the length of the sides of these triangles to range from about 15nm to about 45nm. The amount of atoms in the studied hexagons was in between 2000 – 10000 and in the round flakes about 4900 – 5300.

As it shall be shown in the following first report (appendix A), this extremely simple TB model agrees remarkably well with the results given by the full density functional theory (DFT) calculations. Still it is good to notice that this model does not take into account the possible spin-polarization of the edge states with high degeneracy [12].

4 Summary of Results

After verifying that the used *Hückel* model is applicable in this research (compared to the conventional density functional theory) the following findings and notations were done.

The DOS close to Fermi energy is independent of the size of the triangles and armchair-edged hexagons but depends strongly on the size of the zigzag-edged hexagons and the round flakes. Zigzag-edged triangles have edge states with high density of states at Fermi energy E_f, whereas the armchair-edged triangles have additional set of "ghost states" close to the Fermi energy. These ghost states are results of the interplay between the graphene band structure and the plane wave solution of the wave equation and are distributed evenly in energy. The same ghost states appear in

all the graphene flakes that can be constructed from same sized equilateral armchair triangles with additional rows of atoms in between them. Near the Fermi energy electrons in triangular flakes behave as free massless particles, whereas at the bottom and at the top of the band a supershell structure, similar to that of free electrons in a triangular cavity, is seen. Edge roughness has only a small effect on the level structure of the triangular flakes but this effect is remarkably enhanced on the other types of flakes. Edge roughness was studied by removing a fraction of edge atoms randomly.

Also hexagonal flakes can be constructed to have zigzag or armchair edges. In the case of the armchair edge, the shell structure is distinct and scalable with size (as it is in the case of triangular flakes). But for the zigzag-edged hexagons the shell structure is strongly dependent on the size of the flake.

In the case of the round flakes, a shell structure of a circular cavity could be expected. However, the level structure close to Fermi energy is dominated by edge states that appear in the zigzag regions of the edge. The lengths and distribution of these regions vary with the diameter of the flake and consequently the level structure is very sensitive to the size of the flake.

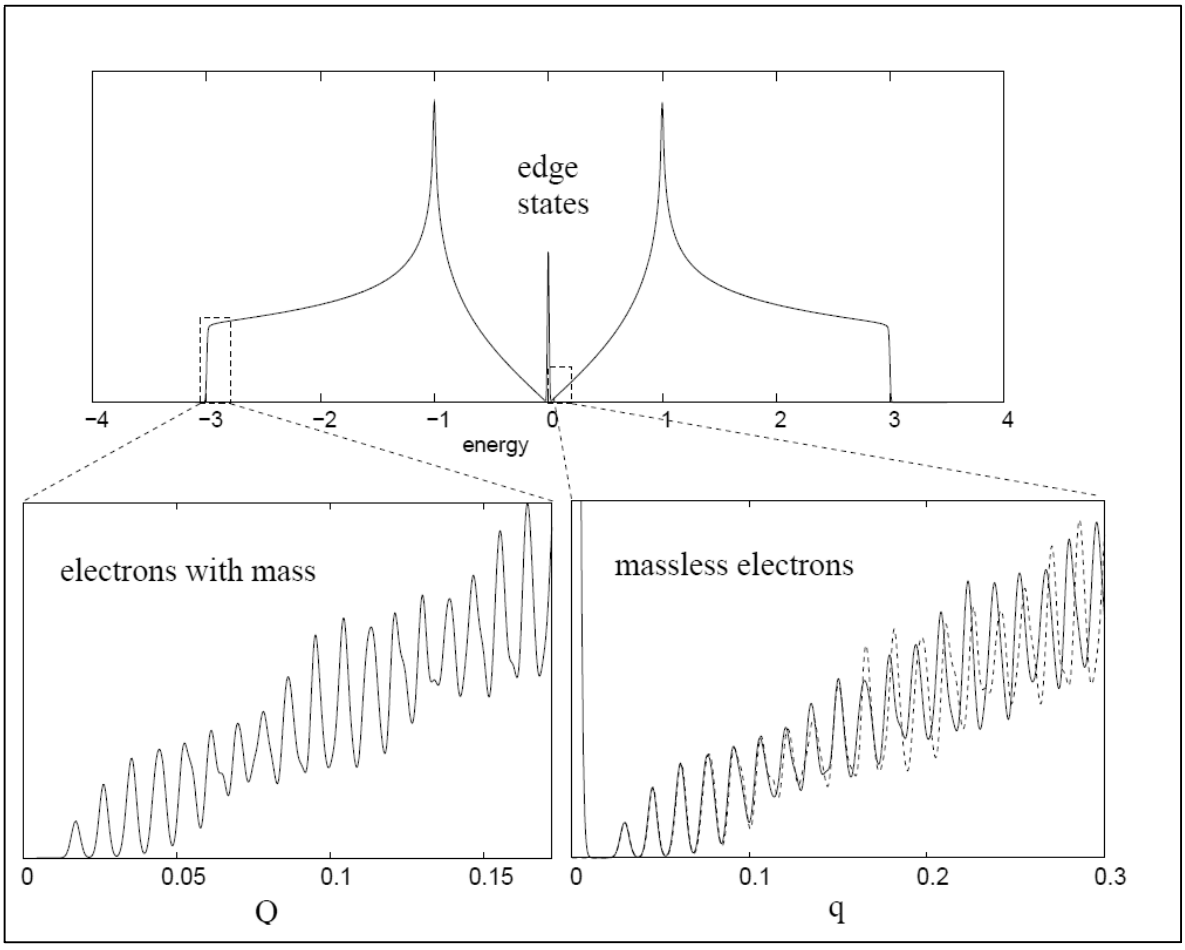

Figure 4: Upper panel: Tight-binding density of states of the largest graphene triangle studied with 44097 atoms and zigzag edges. The discrete energy levels have been smoothened with Gaussians. The peak at zero energy corresponds to the edge states localized at zigzag edges. The lower panels show detailed density of states as a function of the wave number at the bottom of the band (left) and just above the Fermi level (right). The dashed line shows the analytical result for a triangular cavity.

In triangular graphene flakes the shell structure at the bottom of the band, as well as close to the Fermi level, could be described with an analytic solution of particles in a triangular cavity. The only difference was that at the Fermi level the Schrödinger equation had to be replaced with the Klein-Gordon (or Dirac) equation. Figure 4 shows that the solution of the tight-binding model for triangular graphene flakes can indeed be quantitatively described with the analytic model and that in both cases the shell structure has a long wave-length modulation known as the super-shell structure. One of the findings in this thesis was that very large and perfect triangles are needed in order to see the supershell structure close to the Fermi level. The main reason for this is the emerging nonlinearity and anisotropy of the energy bands when the energy increases well above the Fermi energy.

The results of this thesis were obtained for isolated graphene flakes and the interaction with substrate or electric leads, which probably could have effects on the shell structure, have not been considered. It has been shown with transport spectroscopy through semiconductor quantum dots [13], however, that the shell structure calculated for this kind of free dots [14] can actually be captured with weak connections to leads. A more direct measurement of the electronic states would be scanning tunnelling microscopy (STM). It has already been used in studying suspended graphene [15]. So, on a proper surface, it is possible that STM spectroscopy could actually reveal the detailed structures of the electron wave functions got in this theoretical research.

5 Publications and Authors Contributions

[A] Publication A: J Akola, H P Heiskanen and M Manninen, Edge-dependent selection rules in magic triangular graphene flakes, Phys. Rev. B **77**, 193410 (2008).

The author of this thesis has performed all tight-binding computations, made analysis of the results and prepared part of the figures. He has also taken part of writing the manuscript. The density functional computations were made by J. Akola.

[B] Publication B: H P Heiskanen, M Manninen and J Akola, Electronic structure of triangular, hexagonal and round graphene flakes near Fermi level, New J. Phys. **10**, 103015 (2008).

The author is mainly responsible of this paper. He has taken active part in planning the research and the structure of the manuscript. He has made all the computations and analyses needed and written the manuscript.

[C] Publication C: M Manninen, H P Heiskanen and J Akola, Electronic shell and supershell structure in graphene flakes, Eur. Phys. J. D (DOI: 10.1140/epjd/e2008-00282-0)

The author has a small but important contribution to this publication. He has performed the computations for the large, 44000 atom, triangle and some of those for spherical flakes. The author did not take part in writing this publication.

References

[1] S M Reimann and M Manninen, Rev. Mod. Phys. **74**, 1283 (2002).

[2] M Brack, J Blaschke, S C Greagh, A G Magner, P Meier and S M Reimann, Z. Phys. D **40**, 276 (1997).

[3] C Berger, Z M Song, T B Li, X B Li, A Y Ogbazghi, R Feng, Z T Dai, A N Marchenkov, E H Conrad, P N First and W A de Heer, J. Phys. Chem. **108**, 19912 (2004).

[4] K S Novoselov, A K Geim, S V Morozov, D Jiang, Y Zhang, S V Dubonos, I V Grogorieva and A A Firsov, Science **306**, 666 (2004).

[5] S Novoselov, A K Geim, S V Morozov, D Jiang, M I Katsnelson, I V Grogorieva, S V Dubonos and A A Firsov, Nature (London) **438**, 197 (2005).

[6] C Berger, Z M Song, X B Li, X S Wu, N Brown, C Naud, D Mayo, T B Li, J Hass, A N Marchenkov, E H Conrad, P N First, and W. A. de Heer, Science **312**, 1191 (2006).

[7] S Y Zhou, G H Gweon, J Graf, A V Fedorov, C D Spataru, R D Diehl, Y Kopelevich, D H Lee, S G Louie and A Lanzara, Nat. Phys. **2**, 595 (2006).

[8] S R Elliot, *The Physics and Chemistry of Solids*, Wiley, New York, (1998).

[9] D A Areshkin, D Gunlycke and C T White, Nano Lett. **7**, 204 (2007).

[10] K Nakada, M Fujita, G Dresselhaus and M S Dresselhaus, Phys. Rev. B **54**, 17954 - 17961 (1996).

[11] S Okada, Phys. Rev. B **77**, 041408(R) (2008).

[12] Y-W Son, M L Cohen and S G Louie, Nature **444,** 347 (2006).

[13] S D Tarucha, D G Austing, T Honda, R J van der Haage and L Kouwenhoven, Phys. Rev. Lett. **77**, 3613 (1996)

[14] M Koskinen, M Manninen and S M Reimann, Phys. Rev. Lett. **79**, 1389 (1997)

[15] G Li, A Luican and E Y Andrei, arXiv:0803.4016v1 (2008)

Edge-dependent selection rules in magic triangular graphene flakes

J. Akola, H. P. Heiskanen, and M. Manninen
NanoScience Center, Department of Physics, P.O. Box 35, FI-40014 University of Jyväskylä, Jyväskylä, Finland
(Received 20 March 2008; published 27 May 2008)

The electronic shell and supershell structure of triangular graphene quantum dots has been studied using density functional and tight-binding methods. The density functional calculations demonstrate that the electronic structure close to the Fermi energy is correctly described with a simple tight-binding model, where only the p_z orbitals perpendicular to the graphene layer are included. The results show that (i) both at the bottom and at the top of the p_z band, a supershell structure similar to that of free electrons confined in a triangular cavity is seen, (ii) close to the Fermi level, the shell structure is that of free *massless* particles, (iii) triangles with armchair edges show an additional sequence of levels ("ghost states") absent for triangles with zigzag edges while the latter exhibit edge states, and (iv) the observed shell structure is rather insensitive to the edge roughness.

DOI: 10.1103/PhysRevB.77.193410 PACS number(s): 73.21.La, 61.48.De, 81.05.Uw

Recent experimental success in manufacturing single layer graphene flakes on various surfaces[1–4] has made graphene a new playground for theoretical and computational physics,[5–9] and more and more experimental results are emerging.[10–12] Most of the recent interest has been focused in the effects caused by the peculiar band structure of graphite near the Fermi level (ϵ_F): Electrons and holes behave as massless particles (Dirac fermions) due to the linear dispersion relation although their velocity is very small.[13]

The triangular shape of two-dimensional clusters is particularly interesting because, in the case of free electrons, it supports perhaps the most persistent and regular supershell structure of all systems.[14] Furthermore, the triangular shape is preferred in two-dimensional metallic systems[15,16] and in plasma clusters.[17] For tetravalent elements, triangular clusters have been observed in silicon.[18] It is reasonable to expect that such shapes can be observed also for carbon, and this is supported further by the fact that equilateral triangles of graphene can be cut with the two most stable edge structures, the zigzag edge and the armchair edge.

In this Brief Report, we wish to point out that finite graphene flakes (or quantum dots) have an intriguing energy spectrum close to the Fermi level. We have performed electronic structure calculations for triangular graphene flakes using the density functional theory (DFT) for all the valence electrons and a tight-binding (TB) approach that considers only the carbon p_z electrons (Hückel model). Our results show that already in small triangular flakes ($N=300$, $L=5$ nm), the electronic levels close to ϵ_F can be understood as those of free massless electrons confined in a triangular cavity. Especially, we demonstrate that the edge structure has a selective role in the electronic shell structure: The zigzag edge prohibits a whole sequence of localized states *inside* the cluster although it supports edge states. This leads to well-defined edge-dependent selection rules that are based on an analytical model. Recently, Yamamoto *et al.*[19] addressed the presence (absence) of edge states at ϵ_F in zigzag (armchair) triangles of graphene, and the effect on the optical absorption, but the simple principles of the underlying energy spectrum have remained unexplained.

It is well known that the atomic p_z electrons perpendicular to the graphene plane are responsible for the captivating band structure shown in Fig. 1 with the valence and the conduction bands meeting at the corners of the hexagonal Brillouin zone.[20,21] The Fermi surface consists of a discrete set of these points of high-k value, and the resulting density of states (DOS) has a zero weight at ϵ_F. The crossover regions have locally hourglass-like shapes, which results in the linear and isotropic electron dispersion relation in the conduction band ($\epsilon > \epsilon_F = 0$) but only in a small energy interval. Since the atomic p_z electrons are perpendicular to the graphene plane, their interaction with the neighboring atoms does not have any directional dependence and, consequently, they can be described as s-type electrons in the TB model. By neglecting also the differential overlap between atomic sites, the system can be described with the traditional Hückel model

$$H_{ij} = \begin{cases} -t, & \text{if } i,j \text{ nearest neighbors} \\ 0, & \text{otherwise} \end{cases},$$

where the hopping parameter t (resonance integral) determines the width of the bands and the on-site energy is chosen to be $\epsilon_F = 0$. We choose to present our results in units $t=1$. The resulting TB bands (Fig. 1) reaches from -3 to $+3$ (in real graphene, our unit t corresponds to about 2.6 eV).

A conceptual cutting of a finite graphene flake breaks covalent bonds, yielding edges with dangling bonds. We consider the dangling bonds to be passivated, say, with hydrogen. Since the covalent bonding with hydrogen involves sp^2 hybridized orbitals, the passivation is expected to have only a small effect on the perpendicular p_z electron states. Therefore, we neglect this effect in our TB model and follow Areshkin *et al.*[21] and treat the edge atoms in the same footing as bulk atoms. Moreover, we will completely neglect the interaction of graphene with the possible substrate and treat the graphene flake as an isolated two-dimensional cluster or quantum dot. As we shall see, the results of the simple TB model agree well with those of the full DFT calculation.

It has been shown that at the bottom of the valence band, the TB model exactly gives the free electron states for a triangular lattice,[22] and the same is true also for the hexagonal graphene. Consequently, at the bottom (and at the top),

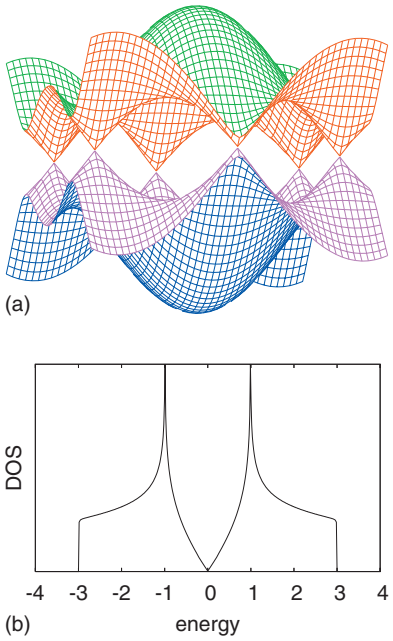

FIG. 1. (Color) Crossover of the valence and conduction bands at the Fermi energy (top) and the density of states (bottom, p_z electrons) of an infinite graphene sheet.

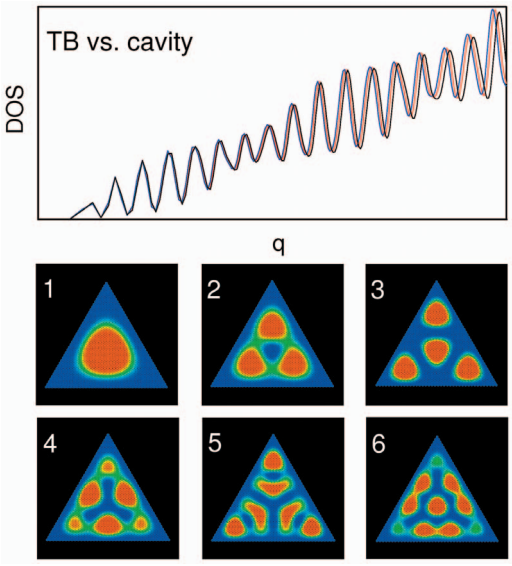

FIG. 2. (Color) Upper panel: DOS at the bottom of the TB band shown as a function of $q=\sqrt{\epsilon+3t}$. Blue: zigzag triangle with 10 000 atoms; red: armchair triangle with 9 918 atoms; and black: result for free electrons in a triangular cavity. Lower panel: Electron densities of the six lowest energy levels.

the energy levels are expected to show the same shell structure as free electrons in a triangular cavity, which is determined by the equation[23,24]

$$\epsilon_{n,m} = \epsilon_0(n^2 + m^2 - nm), \tag{1}$$

where $\epsilon_0 = 8\pi^2\hbar^2/3m_eL^2$, with L being the length of the triangle side. The quantum numbers must satisfy $m \geq 1$ and $n \geq 2m$. Determination of the electron effective mass in the graphene lattice for the TB model gives $\epsilon_0 = 4\pi^2 t/9N$, where N is the number of atoms in the triangle ($L = 3d\sqrt{N}/2$ for a large triangle, d is the nearest-neighbor distance).

The shell structure manifests itself as a regular variation of DOS, which can be determined by the Gaussian convolution of the discrete levels. Figure 2 shows DOS close to the bottom of the valence band obtained from the above equation and compared to the TB model for two graphene triangles, one with 10 000 atoms (zigzag edge) and the other with 9918 atoms (armchair edge). The profiles are clearly similar and exhibit the beating pattern of the supershell structure.[25] Note that DOS is plotted as a function of $\sqrt{\epsilon+3t}$, making the shells equidistant. Figure 2 shows also the electron densities corresponding to the six lowest energy levels (for degenerate states, we show the sum of the density). The density patterns are identical to those of free electrons confined in a triangle[16] or wave modes in triangular resonators.[26]

The Fermi level of graphene consists of two equivalent points at the border of the Brillouin zone (see Fig. 1), where the conduction and valence bands open as circular cones, resulting a linear dispersion relation for electrons $\epsilon(\mathbf{k}) = C\hbar k$, where C is the velocity. Thus, it is to be expected that the electron dynamics is not determined by the Schrödinger equation but by the wave equation of massless particles (or the Dirac equation). For free particles confined in a triangle, the energy levels are still determined by Eq. (1), but now it results in the square of the energy, i.e.,

$$\epsilon_{n,m} = \epsilon_1\sqrt{n^2 + m^2 - nm}, \tag{2}$$

where $\epsilon_1 = 2\pi t/\sqrt{3N}$. It is interesting to note that these energy levels were actually computed for the wave equation much earlier than for the Schrödinger equation.[23]

Figure 3 shows TB-DOS above the Fermi energy for two large triangles ($\sim$10 000 atoms) with zigzag and armchair edges and compares them to the levels of free massless electrons [Eq. (2)]. The results are the following. (i) Each energy level has an additional degeneracy of two due to the two equivalent points at ϵ_F. (ii) The zigzag triangle shows the levels of Eq. (2) with index values $m \geq 1$ and $n \geq 2m$, while the armchair edge shows all the levels where $n \geq m \geq 1$. (iii) The states are much less dense than at the bottom of the band and Eq. (2) describes only the lowest states accurately. (iv) Due to the sparseness of the states, no supershell oscillations are visible for the massless particles (although the supershell structure of ordinary electrons is clearly seen in Fig. 2). (v) The zigzag edge supports particularly visible edge states[27,28] that appear at ϵ_F as a prominent peak. The number of these states equals the number of the outermost edge atoms in zigzag triangles, which is $N_{ss} = \sqrt{N}$.

In order to compare our results to a more realistic calculation, we have performed DFT calculations for triangular $C_{321}H_{51}$ (zigzag) and $C_{330}H_{60}$ (armchair) flakes with the CPMD program.[29] The DFT calculations use a plane wave basis set ($E_{cut} = 50$ Ry), pseudopotentials,[30] and a generalized gradient-corrected Perdew–Burke–Ernzerhof approximation for the exchange-correlation energy.[31] The resulting DFT-DOS of *all* valence electrons is plotted in Fig. 3(b) for both systems, and they show overall features characteristic

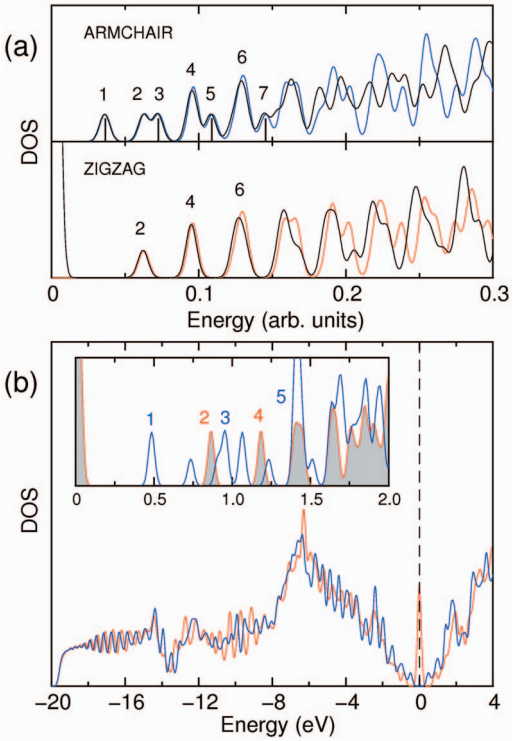

FIG. 3. (Color) Upper panel: TB-DOS at the Fermi level displayed as a function of energy (red and blue curves) compared to the density of levels of Eq. (2) (black curves). The zigzag triangle has 10 000 atoms and the armchair triangle 9918 atoms. Lower panel: DOS of the full DFT calculation for the triangular $C_{321}H_{51}$ (zigzag, red) and $C_{330}H_{60}$ (armchair, blue) flakes. The inset shows the levels above the Fermi surface where the zigzag spectrum is shaded.

for graphite. The zigzag edge states at ϵ_F are visible and the closest conduction states obey the simple analytical model of Eq. (2). The even-numbered peaks are split for the armchair triangle, which is a result reproduced by TB (the splitting reduces with increasing system size).

The lowest conduction states that are labeled in Fig. 3 show fascinating details and the electron densities of two such states are visualized in Fig. 4. For comparison, we show the same states and/or orbitals calculated for a large triangle with the TB model (4920 C atoms) and for a small triangle calculated with the DFT method (330 C atoms). The internal structure (symmetry) of the states is clearly similar, and therefore, it is independent of the triangle size and the model used. The states close to the Fermi level appear very different from those at the bottom of the band (Fig. 2). They are *not* simple densities of massless particles confined in a triangle since the density profile does not decay to zero at the edges. The corresponding electron levels are close to the Brillouin zone boundary, having large k values and the wave functions have pronounced oscillations with wavelengths that are related to the unit cell size. These oscillations guarantee that the wave function will be formally zero at the edges but the corresponding pseudowave function of the massless particle does not necessarily show the same behavior. An interesting feature in Fig. 4 is that the states have simple geometric structure of triangular symmetry. The size (number) of the

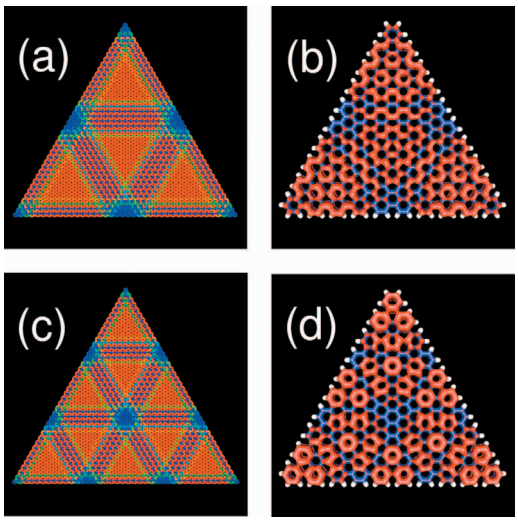

FIG. 4. (Color) Electron density of the [(a) and (b)] third and [(c) and (d)] fifth energy levels above the Fermi energy in armchair triangles (ghost states, labeled in Fig. 3, each has a degeneracy two). (a) and (c) are computed for a large TB triangle of 4920 C atoms, while (b) and (d) are DFT results for a $C_{330}H_{60}$ molecule.

triangles decreases (increases) with increasing energy, i.e., the pattern repeats itself. These "ghost states" are completely absent for the zigzag triangles, and they correspond to quantum numbers of Eq. (2) that are not allowed for free electrons in a triangular box [i.e., $2m \geq n \geq m \geq 1$ in Eq. (2)].

Figure 5 shows the electron densities corresponding to the "normal" low energy states that obey the standard selection rules ($m \geq 1$ and $n \geq 2m$). Again, the electron density does not necessarily vanish at the edges of the triangle. The corresponding states for the armchair and zigzag triangles display obvious differences despite the fact that they involve the same set of quantum numbers (and energy).

Finally, we want to note that a small roughness of the

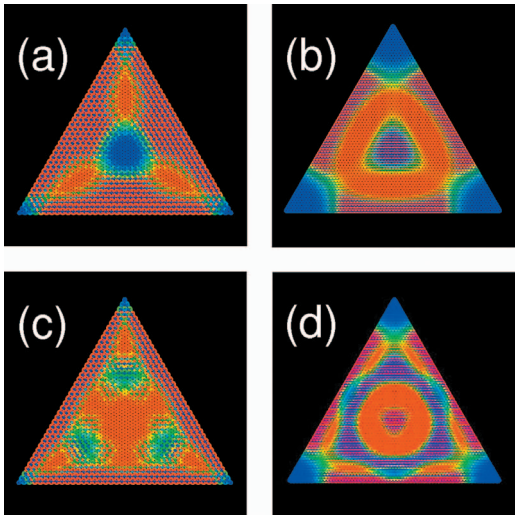

FIG. 5. (Color) Electron density (TB model) of the [(a) and (b)] second and [(c) and (d)] fourth energy levels above the Fermi energy (labeled in Fig. 3) for armchair and zigzag triangles of 4920 and 5181 C atoms, respectively.

edge does not remove the peculiar states shown in Fig. 4 or change the shell structure close to the Fermi level. These ghost states form a triangular network, and it would be interesting to study if they can exist also in the graphene flakes with hexagonal, parallelogram, or trapezoidal shapes.

In conclusion, we have computed the electronic structure of triangular graphene flakes and shown that the DOS profile close to ϵ_F is independent of the triangle size, and it can be described with the simple TB model. The zigzag flakes exhibit well-known edge states and the armchair triangles show an additional set of ghost states (different selection rules) where the corresponding electron density makes a triangular pattern. In large triangles of 5000–10 000 C atoms, the energy levels can be accurately described by considering free massless particles confined in a triangular cavity. Presumably, the electronic states near the Fermi surface are not sensitive to the dielectric substrate, and we expect that these fascinating wave functions can be observed with scanning tunneling microscopy.

This work has been supported by the Academy of Finland. The DFT calculations were performed on IBM-SP4+ platforms at the John von Neumann Institute for Computing (NIC), Forschungszentrum Jülich, Germany.

[1] C. Berger, Z. M. Song, T. B. Li, X. B. Li, A. Y. Ogbazghi, R. Feng, Z. T. Dai, A. N. Marchenkov, E. H. Conrad, P. N. First, and W. A. de Heer, J. Phys. Chem. **108**, 19912 (2004).
[2] K. S. Novoselov, A. K. Geim, S. V. Morozov, D. Jiang, Y. Zhang, S. V. Dubonos, I. V. Grigorieva, and A. A. Firsov, Science **306**, 666 (2004).
[3] K. S. Novoselov, A. K. Geim, S. V. Morozov, D. Jiang, M. I. Katsnelson, I. V. Grigorieva, S. V. Dubonos, and A. A. Firsov, Nature (London) **438**, 197 (2005).
[4] C. Berger, Z. M. Song, X. B. Li, X. S. Wu, N. Brown, C. Naud, D. Mayo, T. B. Li, J. Hass, A. N. Marchenkov, E. H. Conrad, P. N. First, and W. A. de Heer, Science **312**, 1191 (2006).
[5] J. Alicea and M. P. A. Fisher, Phys. Rev. B **74**, 075422 (2006).
[6] V. P. Gusynin and S. G. Sharapov, Phys. Rev. Lett. **95**, 146801 (2005).
[7] V. P. Gusynin, S. G. Sharapov, and J. P. Carbotte, Phys. Rev. Lett. **96**, 256802 (2006).
[8] K. Nomura and A. H. MacDonald, Phys. Rev. Lett. **98**, 076602 (2007).
[9] Y.-W. Son, M. L. Cohen, and S. G. Louie, Phys. Rev. Lett. **97**, 216803 (2006).
[10] K. S. Novoselov Z. Jiang, Y. Zhang, S. V. Morozov, H. L. Stormer, U. Zeitler, J. C. Maan, G. S. Boebinger, P. Kim, and A. K. Geim, Science **315**, 1379 (2007).
[11] A. K. Geim and K. S. Novoselov, Nat. Mater. **6**, 183 (2007).
[12] G. Li and E. A. Andrei, Nat. Phys. **3**, 623 (2007).
[13] S. Y. Zhou, G. H. Gweon, J. Graf, A. V. Fedorov, C. D. Spataru, R. D. Diehl, Y. Kopelevich, D.-H. Lee, S. G. Louie, and A. Lanzara, Nat. Phys. **2**, 595 (2006).
[14] M. Brack, J. Blaschke, S. C. Greagh, A. G. Magner, P. Meier, and S. M. Reimann, Z. Phys. D: At., Mol. Clusters **40**, 276 (1997).
[15] J. Kolehmainen, H. Häkkinen, and M. Manninen, Z. Phys. D: At., Mol. Clusters **40**, 306 (1997).
[16] E. Janssens, H. Tanaka, S. Neukermans R. E. Silverans, and P. Lievens, New J. Phys. **5**, 46 (2003).
[17] S. M. Reimann, M. Koskinen, J. Helgesson, P. E. Lindelof, and M. Manninen, Phys. Rev. B **58**, 8111 (1998).
[18] M. Y. Lai and Y. L. Wang, Phys. Rev. Lett. **81**, 164 (1998).
[19] T. Yamamoto, T. Noguchi, and K. Watanabe, Phys. Rev. B **74**, 121409(R) (2006).
[20] S. R. Elliot, *The Physics and Chemistry of Solids* (Wiley, New York, 1998).
[21] D. A. Areshkin, D. Gunlycke, and C. T. White, Nano Lett. **7**, 204 (2007).
[22] M. Manninen, J. Mansikka-aho, and E. Hammarén, Europhys. Lett. **15**, 423 (1991).
[23] F. E. Borghis and C. H. Papas, in *Encyclopedia of Physics*, edited by S. Flücke (Springer, Berlin, 1957).
[24] H. R. Krishnamurthy, H. S. Mani, and H. C. Verma, J. Phys. A **15**, 2131 (1982).
[25] S. M. Reimann, M. Koskinen, H. Häkkinen, P. E. Lindelof, and M. Manninen, Phys. Rev. B **56**, 12147 (1997).
[26] Y.-Z. Huang, W.-H. Guo, L.-J. Yu, and H.-B. Lei, IEEE J. Quantum Electron. **37**, 1259 (2001).
[27] K. Kobayashi, Phys. Rev. B **48**, 1757 (1993).
[28] K. Nakada, M. Fujita, G. Dresselhaus, and M. S. Dresselhaus, Phys. Rev. B **54**, 17954 (1996).
[29] CPMD Version 3, 11 Copyright IBM Corp., 1990–2006, Copyright MPI für Festkörperforschung Stuttgart 1997–2001 (www.cpmd.org).
[30] N. Troullier and J. L. Martins, Phys. Rev. B **43**, 1993 (1991).
[31] J. P. Perdew, K. Burke, and M. Ernzerhof, Phys. Rev. Lett. **77**, 3865 (1996).

New Journal of Physics
The open-access journal for physics

Electronic structure of triangular, hexagonal and round graphene flakes near the Fermi level

H P Heiskanen, M Manninen[1] and J Akola
Nanoscience Center, Department of Physics, PO Box 35,
FI-40014 University of Jyväskylä, Finland
E-mail: matti.manninen@jyu.fi

New Journal of Physics **10** (2008) 103015 (14pp)
Received 13 June 2008
Published 10 October 2008
Online at http://www.njp.org/
doi:10.1088/1367-2630/10/10/103015

Abstract. The electronic shell structure of triangular, hexagonal and round graphene quantum dots (flakes) near the Fermi level has been studied using a tight-binding method. The results show that close to the Fermi level the shell structure of a triangular flake is that of free *massless* particles, and that triangles with an armchair edge show an additional sequence of levels ('ghost states'). These levels result from the graphene band structure and the plane wave solution of the wave equation, and they are absent for triangles with a zigzag edge. All zigzag triangles exhibit a prominent edge state at ϵ_F, and few low-energy conduction electron states occur both in triangular and hexagonal flakes due to symmetry reasons. Armchair triangles can be used as building blocks for other types of flakes that support the ghost states. Edge roughness has only a small effect on the level structure of the triangular flakes, but the effect is considerably enhanced in the other types of flakes. In round flakes, the states near the Fermi level depend strongly on the flake radius, and they are always localized on the zigzag parts of the edge.

[1] Author to whom any correspondence should be addressed.

Contents

1. Introduction

Nearly free electrons trapped by a high-symmetry potential exhibit a shell structure that arises from the symmetry-induced degeneracy and bunching of energy levels of different radial modes. Such a level structure has been observed in metallic clusters and semiconductor quantum dots (for reviews see [1, 2]). Usually, the shell structure is associated with a spherical or circular symmetry, but it exists also, for example, in three-dimensional icosahedral [3] and two-dimensional triangular clusters [4]. The shell structure is a single-particle property and can be understood on the basis of the jellium model of delocalized electrons [5] or the tight-binding (TB) approach [6].

In two-dimensional systems, the most interesting confinement geometries for electrons are a circle, hexagon and triangle. Obviously, the circle has the highest symmetry of these and the triangle the lowest. Surprisingly, however, it is the triangle that has the most persistent shell structure and also a regular supershell structure [7]. The triangular shape is preferred in two-dimensional metallic systems [4, 8, 9], in plasma clusters [10], and it is observed also in semiconducting silicon clusters [11].

The shell structure of quantum dots and metal clusters is caused by nearly free conduction electrons. In the case of graphene, the situation is different due to the peculiar band structure. The Fermi surface consists of a set of discrete points, and the electron (hole) dispersion relation of the conduction (valence) band is linear. Recent experiments have shown that nanometre-sized graphene flakes can be produced on various surfaces [12]–[18], which has induced a significant amount of theoretical interest [19]–[30].

In this paper, we show that finite graphene flakes (or quantum dots) have an interesting energy spectrum close to the Fermi level. The most common edges of graphene are the so-called armchair and zigzag edges. It turns out that the energy spectrum of graphene flakes depends strongly on the type of the edge, and that flakes of similar size and shape can exhibit distinctly different electronic structure (selection rules). In an earlier report [31], we reported results for triangular graphene flakes and showed that a simple TB model that considers only the carbon p_z electrons produces a similar shell structure to a full electronic structure calculation with all the valence electrons (based on density functional theory, (DFT)). Moreover, the results showed that the electronic levels close to the Fermi energy can be understood as those of free massless electrons confined in a triangular cavity. Herein, we shall further investigate the peculiarities of the graphene electronic structure that are caused by the geometry and edge structure of the flake.

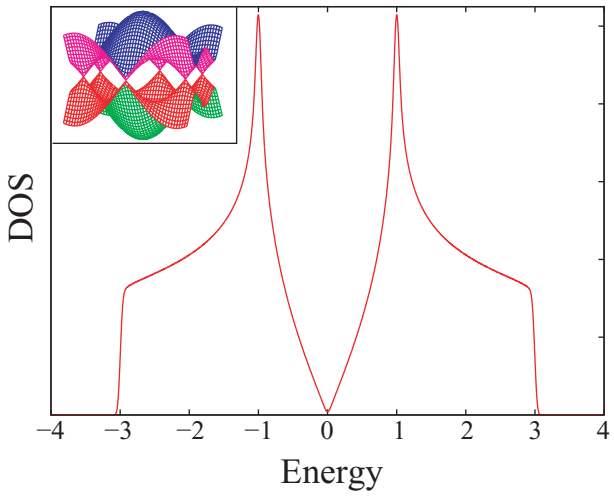

Figure 1. The DOS (p_z electrons) of an infinite graphene sheet for the TB method used. Inset: cross-over of the valence and conduction bands at the Fermi energy.

The atomic p_z electrons perpendicular to the graphene plane are responsible for the band structure shown in figure 1, where the valence and the conduction bands meet at the corners of the hexagonal Brillouin zone [32, 33]. The Fermi surface consists of a discrete set of these points of high-k value, and the resulting density of states (DOS) has a zero weight (as well as zero band gap) at the Fermi energy ϵ_F. The dispersion relation is linear in the near vicinity of the Fermi level. Since the atomic p_z electrons are perpendicular to the graphene plane their interaction with the neighboring atoms does not have any directional dependence and the TB model can be reduced to the traditional Hückel model

$$H_{ij} = \begin{cases} -t, & \text{if } i, j \text{ nearest neighbors,} \\ 0, & \text{otherwise,} \end{cases} \tag{1}$$

where the hopping parameter t (resonance integral) determines the width of the bands and the on-site energy is chosen to be $\epsilon_F = 0$. We present our results in units $t = 1$ (in real graphene our unit t corresponds to about 2.6 eV). It is important to note that the simple TB model becomes equivalent to that of the free electron model when the electron wavelength becomes much larger than the interatomic distance [6]. This is valid at the bottom of the valence band where the free electron model gives the correct shell and supershell structure [31]. The situation is more complicated near the Fermi level where the electron wavelength ascribes to the interatomic distance. However, as we shall see, also there the level structure can be understood in terms of the free electron model, but now for *massless* electrons.

In the following, we consider graphene flakes that are cut out from a perfect infinite graphene sheet and neglect the effects of the substrate as well as the passivation of dangling bonds. The passivation, say with hydrogen, involves sp^2 hybridized orbitals and is expected to have only a marginal effect on the perpendicular p_z electron states [32, 33]. This approximation was supported by our earlier work where we compared the full DFT calculations of hydrogen passivated graphene flakes with the results of the simple Hückel model without passivation [31]. Note, however, that our simple model cannot account for possible spin-polarization of the edge states with large degeneracy [34].

2. Triangular graphene flakes

The Fermi level of graphene consists of two equivalent points at the border of the Brillouin zone (see figure 1) where the conduction and valence bands open as circular cones resulting in a linear dispersion relation for electrons $\epsilon(\mathbf{k}) = C\hbar k$, where C is the velocity. Thus, it is to be expected that the electron dynamics is not determined by the Schrödinger equation but by the equation of massless particles (Klein–Gordon or Dirac equation). The simple wave equation for a triangular cavity has an analytic solution [35] which gives the energy eigenvalues

$$\epsilon_{n,m} = \epsilon_1 \sqrt{n^2 + m^2 - nm}, \tag{2}$$

where m and n are positive integers with $n \geqslant 2m$. The state with $n = 2m$ is nondegenerate, whereas states with $n > 2m$ have a degeneracy 2. In our case $\epsilon_1 = 2\pi t/\sqrt{3N}$, N being the number of atoms. In the case of the Schrödinger equation (i.e. electrons with mass), the exact solution gives $\epsilon \propto n^2 + m^2 - nm$, i.e. equation (2) without the square root. It is interesting to note that the exact solution for the wave equation was presented by Lame already in 1852 [36], as noted by Krishnamurthy who studied the corresponding solution of the Schrödinger equation [37]. The corresponding wave functions can be found in [38].

The eigenvalues of equation (2) are solutions of the wave equation for massless particles, for example, for elastic waves, for electromagnetic waves or for the positive energy solutions of the Klein–Gordon equation. We want to emphasize that we have not shown that they are solutions of the Dirac equation where the boundary conditions are tricky for a cavity [21, 30, 39]. However, our numerical solutions of the TB problem for large triangular flakes are in excellent agreement with those of equation (2).

The electronic DOS of a finite system (flake) consists of a set of discrete energy levels. Instead of plotting the level structure it is more useful to study the density of levels since it points out more clearly the exact and nearly exact degeneracies of levels as well as the shell structure, which manifests itself as a regular variation of the level density. It is thus useful to define a continuous DOS by using a Gaussian convolution of the discrete levels ϵ_i:

$$g(\epsilon) = \frac{1}{\sigma\sqrt{2\pi}} \sum_i \mathrm{e}^{-(\epsilon-\epsilon_i)^2/2\sigma^2}, \tag{3}$$

where σ is the width of the Gaussian.

Figure 2 shows TB-DOS above the Fermi energy for three graphene triangles (∼22 000, 15 000 and 5600 atoms) with armchair and zigzag edges and compares them with the DOS of free massless electrons (see equation (2)). For armchair flakes, the comparison includes now additional (forbidden) index values $m = n$. The results are the following: (i) each energy level has an additional degeneracy of two due to the two equivalent points at ϵ_F. (ii) The zigzag triangle shows the levels of equation (2) with index values $m \geqslant 1$ and $n \geqslant 2m$, whereas the armchair edge shows also those where $n = m$. We call these additional states (where $n = m$) 'ghost states'. (iii) Equation (2) describes only the lowest states accurately and is more successful for larger triangles. (iv) Due to the sparseness of the states, supershell oscillations of the massless particles become visible only in the large triangles (although they are already visible at the bottom of the band in small triangles [31]). (v) The zigzag edge supports particularly visible edge states [41, 42] that appear at ϵ_F as a prominent peak (figure 2). The number of these states equals the number of the outermost edge atoms in zigzag triangles, which is $N_{ss} = \sqrt{N}$. We shall return to the edge states in section 6.

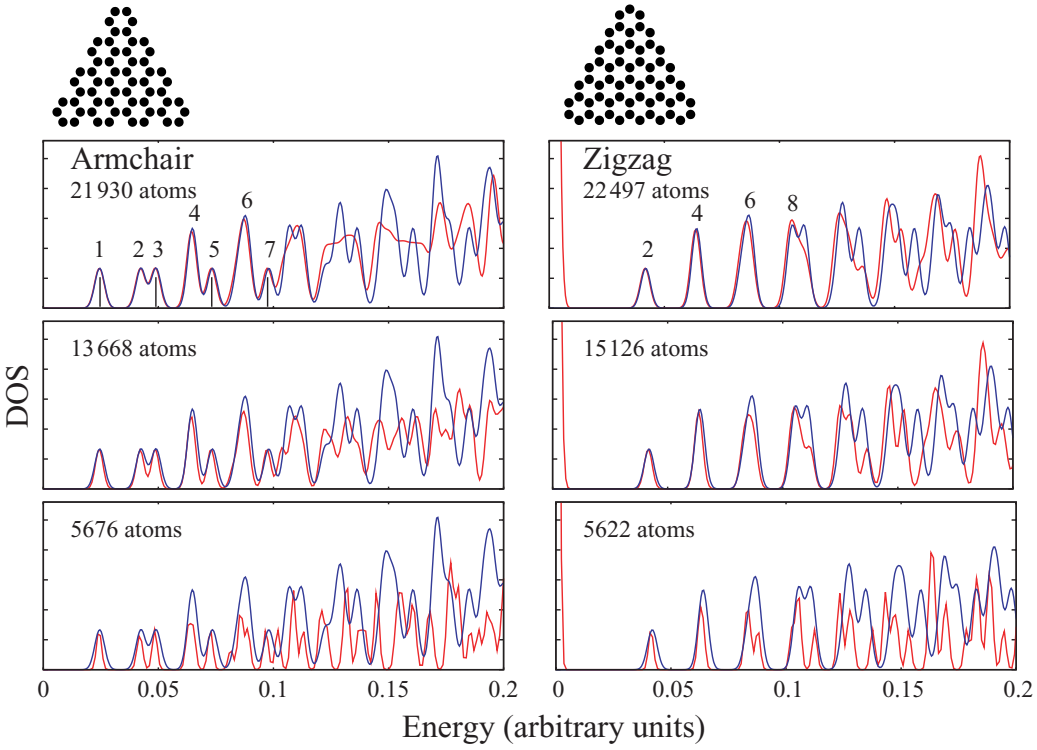

Figure 2. TB-DOS above the Fermi energy for triangular flakes (red curves), compared to the DOS of equation (2) (blue curves). The sizes of the triangles are given as numbers of atoms. Note that the triangles showing the geometries are much smaller. The energy is in units of t for the largest armchair and zigzag triangles, respectively. For the smaller sizes, the energy has been scaled by the square root of the number of atoms in order to get the peaks at the same positions.

Graphene ribbons with armchair edge show DOS with or without a gap, depending on width of the ribbon [42]. In the case of triangular flakes with armchair edges no such effect was seen. The only size dependence observed was the scaling of the energy levels with the flake size.

The lowest conduction states that are numbered in figure 2 show fascinating details, and the electron densities of such states are visualized in figure 3. The abovementioned ghost states (left, labeled by odd indices) show an interesting feature as they have a simple geometric pattern of triangular symmetry. The size (number) of the triangles decreases (increases) with increasing energy, i.e. the pattern repeats itself. These ghost states are completely absent for the zigzag triangles, and they correspond to quantum numbers of equation (2) not allowed for free electrons in a triangular box (i.e. $n = m$ (with extra degeneracy) in equation (2)). Previously, we calculated the same states for a smaller armchair triangle with a DFT method (330 C atoms, 60 passivating H atoms) [31]. The internal structure (symmetry) of the states was clearly similar, and therefore, the phenomenon is independent of the triangle size and the model used. We shall discuss the ghost states in detail in section 4.

Figure 3 (right) shows the electron densities corresponding to the 'normal' low energy states that obey the standard selection rules ($m \geqslant 1$ and $n \geqslant 2m$). Again, the electron density does not necessarily vanish at the edges of the triangle. Interestingly, the corresponding states

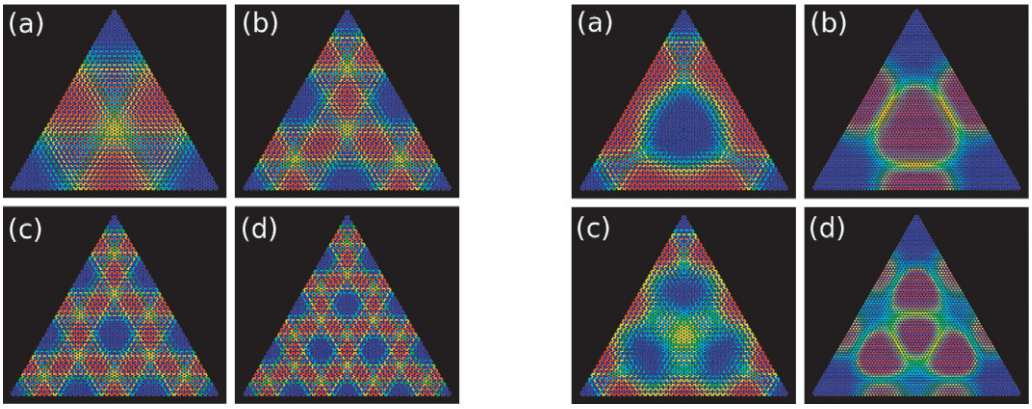

Figure 3. LEFT FOUR: electron density of (a) the 1st, (b) 3rd, (c) 5th and (d) 7th energy levels above the Fermi energy in armchair triangles ('ghost states', labeled in figure 2). Each level has a degeneracy of two. RIGHT FOUR: electron density of ((a) and (b)) the 2nd and ((c) and (d)) the 4th energy levels above the Fermi energy (labeled in figure 2) for armchair and zigzag triangles of 4920 and 5181 C atoms, respectively. Color scale from blue to red, blue corresponds to vanishing density. Each figure shows the sum of the densities of the degenerate states.

for the armchair and zigzag triangles (with the same energy and quantum numbers n and m) display nearly an anticorrelation: the maxima in zigzag triangles are minima in armchair triangles and vice versa. Overall, the states close to the Fermi level appear very different from those at the bottom of the band. They are *not* simple densities of massless particles confined in a triangular cavity since the density profile does not decay to zero at the edges. The corresponding electron levels are close to the Brillouin zone boundary, having large k-values, and the wave functions have pronounced oscillations with wavelengths that are related to the hexagonal unit cell size. These oscillations enable the wave function to be formally zero at the edges, but the corresponding pseudowave function of the massless particle does not necessarily vanish.

3. Hexagonal graphene flakes

Similar TB calculations were performed for hexagonal graphene flakes with armchair and zigzag edges. The comparison between hexagonal and triangular flakes is based on hexagons that were cut from the corresponding triangles (taking the corners off). In general, the level structure is more complicated but some similarities with the triangular flakes can be found. We observe the following results: (i) the zigzag edge supports edge states (see section 6), whereas the armchair edge results in a gap at ϵ_F. (ii) The electron DOSs *near* ϵ_F display the main amplitude at the edges/corners both for the zigzag and armchair edges. (iii) For the zigzag flake, the number of states near the Fermi level depends on the size of the flake. (iv) Hexagonal flakes display few states that have exactly the same electron density as the original triangles (cutting off the corners). (v) In most cases, the electron densities are different than in the corresponding triangular flakes or hexagons with the other type of edge. It is also worth mentioning that at the bottom of the valence band the (p_z) electrons act as free particles not seeing the atomic lattice, which is a case similar to triangles. This makes the supershell structure visible at the bottom of the valence band, but it is not as clear as in the triangular graphene flakes.

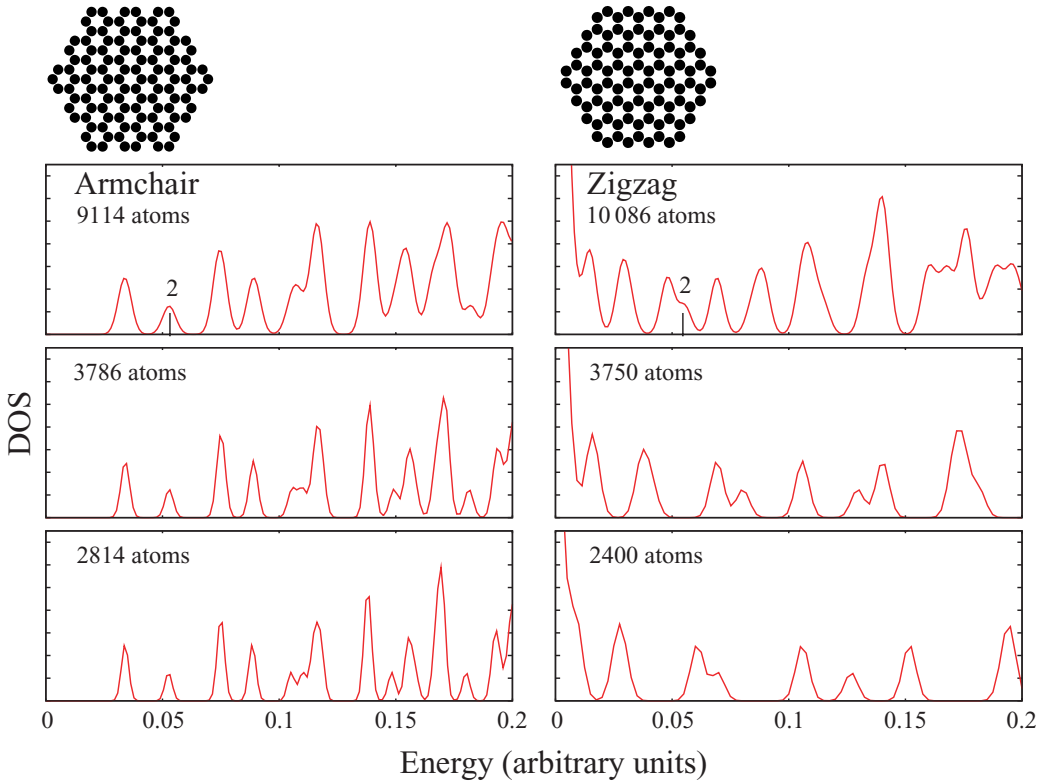

Figure 4. TB-DOS of the hexagonal flakes with armchair (left panel) and zigzag (right panel) edge. The energy is in units of t for the largest hexagons. For the smaller sizes, the energy has been scaled by the square root of the number of atoms (scaling factor $= \sqrt{N_1/N_2}$, where N_1 is the number of atoms in flake 1 and N_2 atoms in flake 2). The geometries are shown as small hexagons.

Figure 4 shows the DOS of hexagonal flakes. In the armchair panel (left), the DOS has been scaled by size in order to get the peaks to coincide near the Fermi level. The scaling factor $\sqrt{N_1/N_2}$ is the same as in the case of triangles. In the zigzag flakes, the scaling does *not* bring the peaks at the same positions. This is a special feature that does not exist in triangular flakes. In general, the zigzag flakes have a peak and the armchair flakes display a gap at ϵ_F, which is the case for triangles also. The hexagonal armchair flakes display states near the Fermi level that are in a sense universal: they do not depend on the size of the flake (cf triangles, figure 2). The armchair flakes do not exhibit any states that could be regarded as ghost states suggesting that these are characteristic for the armchair triangles only. However, as will be shown in section 4, a slight modification of the hexagonal flakes changes the situation. We also note that the DOS near the Fermi energy has some peaks that coincide with the ones of the triangles, and there is one state that is common in all the triangular and hexagonal flakes: the peak '2' in figures 2 and 4. Furthermore, the states that have exactly the same energies in armchair triangles and hexagons display similar electron densities due to the common symmetry properties (figures 5(e) and (f)).

4. Ghost states

The hexagonal armchair flakes of section 3 do not exhibit the peculiar ghost states. The reason is that our flakes obey the armchair construction exactly: the corners are those of a perfect

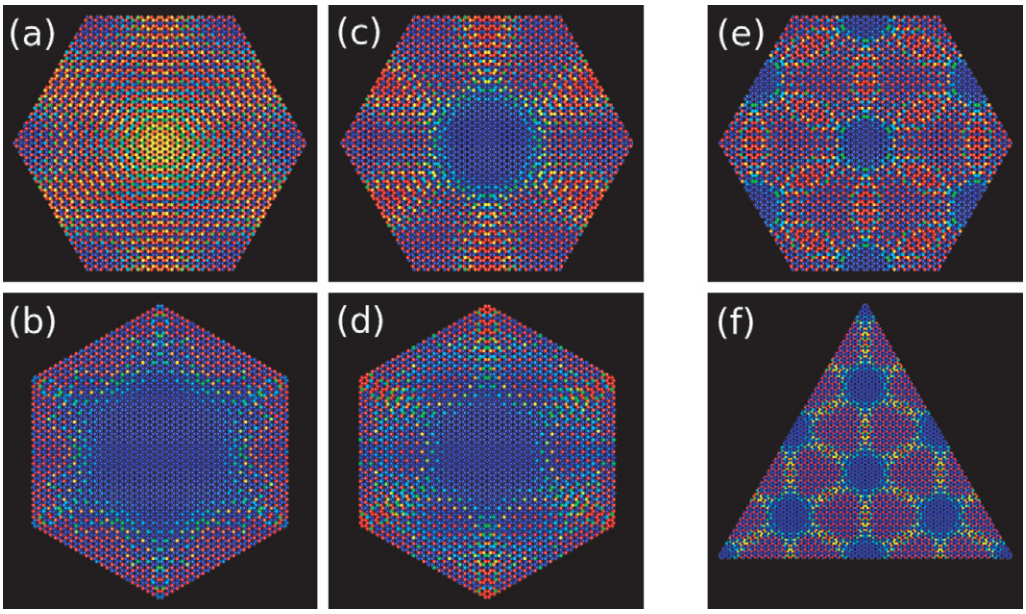

Figure 5. Electron density corresponding ((a) and (b)) the first peak before the peak '2' in figure 4) and ((c) and (d)) the peak '2' for the armchair (upper) and zigzag (lower) hexagons. (e) and (f) show a state that occurs both in the armchair-edged hexagon and triangle (peak '6' in figure 2). Color scale from blue to red, blue corresponds to vanishing density.

honeycomb pattern. However, the ghost states will reappear if the flakes are built differently. This can be understood by studying a triangular armchair flake with ghost states (figures 6(a) and (b)). The boundary conditions of the TB problem require that the wave function is zero at the (imaginary) lattice sites just outside the triangle. Now, we can put two triangles together as in the rhombus-shaped flake shown in figure 6(c)), and add an additional row of atoms between the triangles. This system has naturally the same ghost states as the original triangle. Similarly, we can construct hexagonal flakes with ghost states as shown in figure 6(d), and it is clear that any shape consisting of equilateral triangles can exhibit ghost states. The only requirement is that an additional row of lattice sites (atoms) is added at the interface of the triangles. The ghost states in different triangles are then completely decoupled although they appear as continuous wave functions, and the wave function is exactly zero at the interface. This is also the reason why the ghost state pattern repeats itself: the high-index (large $n = m$) ghost states are the same in large triangles as the low-index ghost states in small triangles, and the energy is exactly the same if the side length L of the large triangle is commensurate with that of the small triangle.

At this point, it is important to note that the hexagonal flakes constructed according to the prescription above do not have perfect corners. Instead of the armchair edge just bending over, they have a small region of zigzag edge at the corners. Similarly, the extra row of atoms in the rhombus shown in figure 6 results in the corners not following the armchair construction. The ghost states disappear if the rhombus is made by merging two triangles together without an additional row of atoms.

The appearance of ghost states in the TB model reflects the balance between the graphene band structure and the free electron states in two-dimensional systems. Figure 6(e) shows the

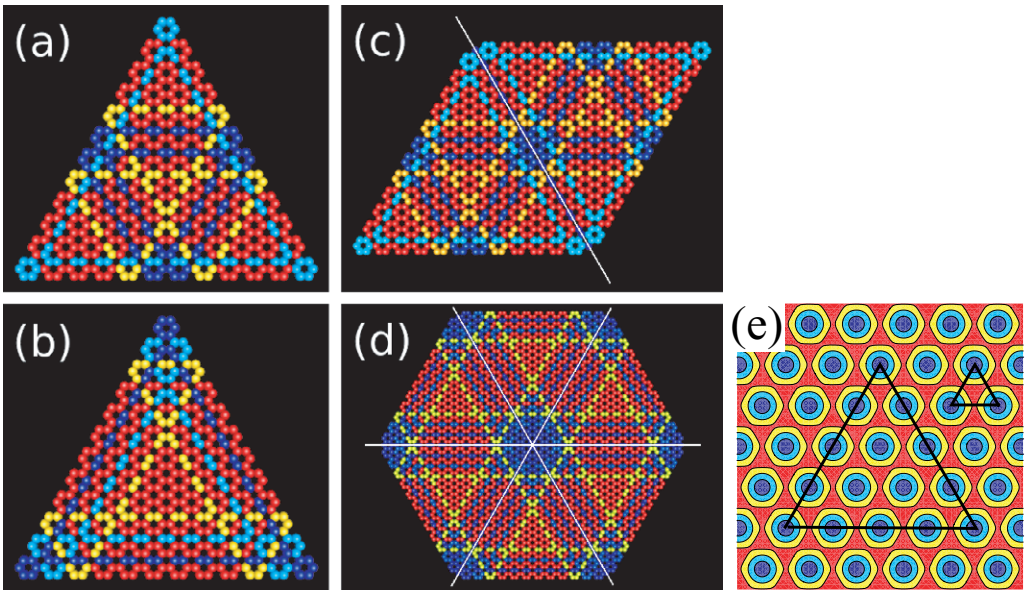

Figure 6. Ghost states in ((a) and (b)) armchair triangles, and the corresponding ghost states (2nd and 1st) in (c) an imperfectly built rhombus and (d) hexagon. The extra rows of atoms are marked with the narrow white lines. (e) shows a standing wave solution of the wave equation in an infinite two-dimensional (hexagonal) system. The small and large triangles in (e) demonstrate how the ghost states (1st and 4th) appear in triangular flakes.

combined density of two degenerate plane waves for free electrons, which can be expressed as

$$n(x, y) = \sin^2 qx + \sin^2\left(\tfrac{1}{2}qx + \sqrt{3}qy\right) + \sin^2\left(\tfrac{1}{2}qx - \sqrt{3}qy\right). \quad (4)$$

This density has a clear similarity of that of the ghost states, except that the rapid oscillations from atom to atom are absent. Again, we want to remind readers that the (pseudo) wave function of these 'Dirac fermions' above the Fermi energy does not need to be zero at the edge of the triangular cavity since the rapid oscillations take care of this boundary condition. Thus, also solutions where the derivative of the pseudowave function is zero are allowed.

5. Edge roughness

The effect of edge roughness was studied for triangular and hexagonal flakes. We removed randomly 10, 38 or 50% of edge atoms and studied how it affected the DOS and electron densities of the states near ϵ_F. The atom removal process avoided situations where the possible remaining atom had only one nearest-neighbor, and such atoms were taken out.

The results are collected in figure 7 which shows the TB-DOS above the Fermi energy (upper panel) and the electron density of the 2nd conduction electron state (peak '2', lower panel). Especially in the case of hexagonal flakes, the edge roughness has a noticeable effect on DOS and electron densities. Already a small edge roughness causes the degeneracy of the states to break up, and for example, removal of only 10% of edge atoms in the zigzag-edged hexagonal flake results in a significant perturbation, and the electron density pattern of the intact

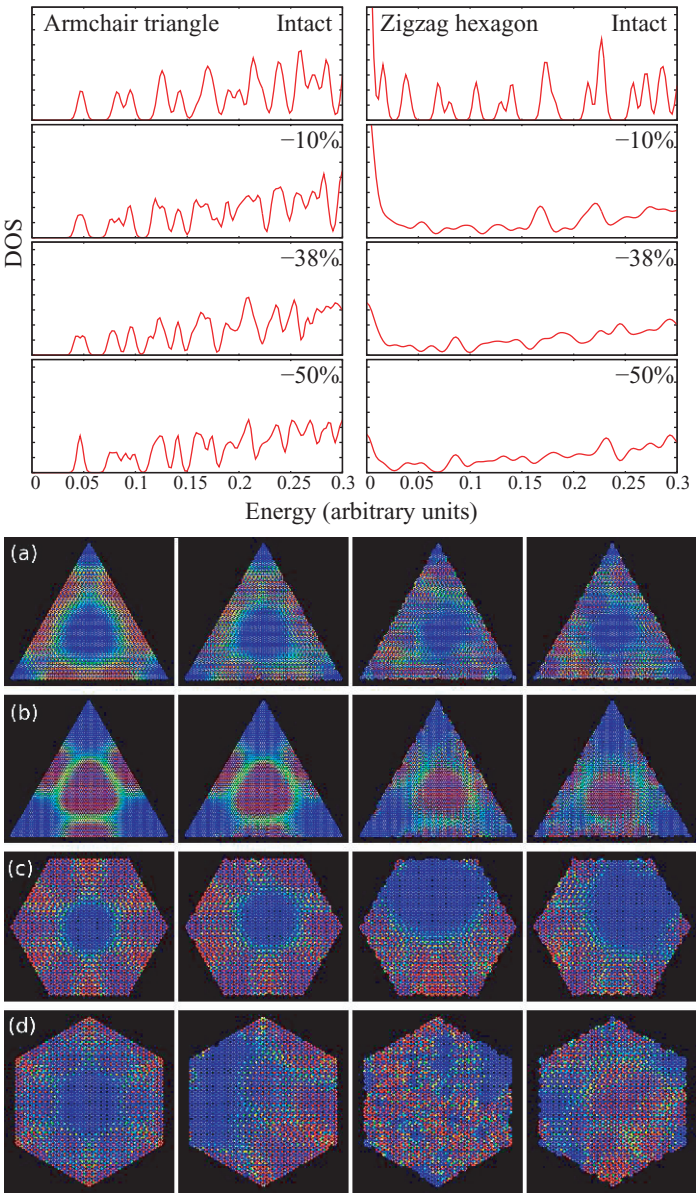

Figure 7. Upper panels: effect of the edge roughness on TB-DOS for an armchair triangle (left) and zigzag hexagon (right). Lower panels: effect of the edge roughness on the electron density of the 2nd conduction electron state for armchair and zigzag flakes. Triangular flake with (a) armchair edge and (b) zigzag edge. Hexagonal flake with (c) armchair edge and (d) zigzag edge. From left to right: intact edge, 10, 38, and 50 percent of the edge atoms removed. Color scale from blue to red, blue corresponds to vanishing density.

flake cannot be identified anymore. The changes are less dramatic for triangular flakes, and the pattern of the 2nd conduction state is always recognizable. The DOS curves indicate that the states closest to ϵ_F are the most robust against edge roughness. Finally, the electron density of the corresponding states seems to avoid the rough parts of the edge in the case of armchair edge and favor them in the case of zigzag edge.

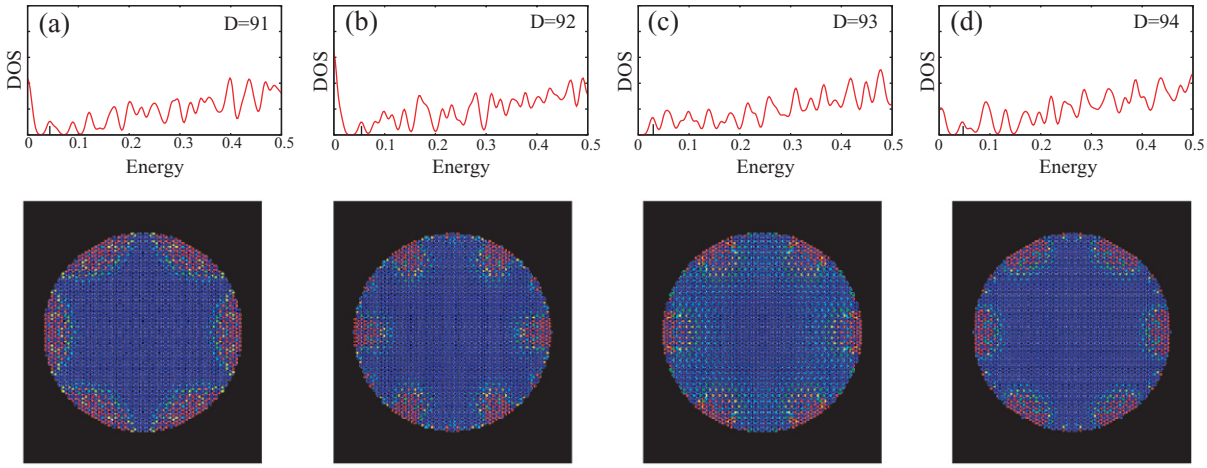

Figure 8. TB-DOS of round graphene flakes (upper panel) and electron densities (lower panel) of the first conduction electron state above ϵ_F (marked with a tick in the DOS panels). The flake diameters (D) are (left to right): 91, 92, 93, and 94 times the nearest-neighbour distance corresponding to 4980, 5118, 5238, and 5338 atoms, respectively. Color scale from blue to red, blue corresponds to vanishing density.

6. Round graphene flakes

Finally, we have studied round (circular) graphene flakes. Round flakes were cut out of a graphene sheet as follows: the center was chosen to be a high-symmetry point (an atom or a center of a hexagon), and all the atoms inside a chosen radius were included. After this, all the edge atoms with only one nearest-neighbour were removed. The number of atoms is thus determined by the chosen radius and center. Figure 8 shows the TB-DOS above the Fermi level for four round graphene flakes with almost the same diameter and ∼5000 atoms. Based on the triangular and hexagonal graphene flakes, one might expect that the shell structure is independent of the size. Figure 8 demonstrates that this is clearly not the case. On the contrary, the level structure is very sensitive to the flake diameter. This can be understood by inspecting the structure of the low-energy wave functions (lower panel in figure 8). The states above the Fermi energy are localized close to the flake edges, and therefore, they experience the detailed edge geometry.

The edge of a circular flake comprises not only the simple armchair and zigzag segments, but also more complicated parts. Figure 8 shows the electron density of the lowest state above the Fermi level. In all cases, the electron density is concentrated in the zigzag regions. The length and distribution of the zigzag segments vary with the flake diameter (size). This causes the energy of the corresponding state to be different for each round flake. The same argument applies for all the low-energy states since they have marked amplitudes at the edges, and it explains the strong size-dependence of DOS. The edge states have large degeneracy (or near degeneracy) as seen as a large peak at zero energy in the plots of the DOS in figures 2, 4 and 8(b). This can cause spin-polarization in a partially filled case due to Hund's first rule, but this is out of the reach of our simple model.

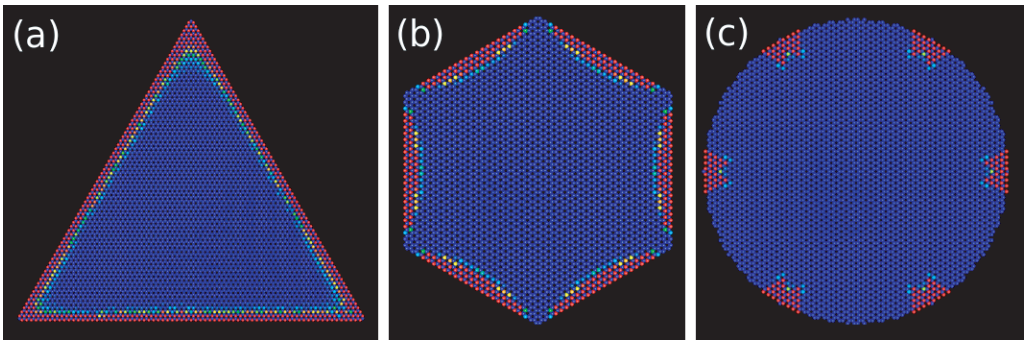

Figure 9. Electron density of the edge states (DOS peak at ϵ_F) for (a) a zigzag triangle (5622 atoms, 72 states), (b) zigzag hexagon (3750 atoms, 18 states), and (c) round flake (5118 atoms, 12 states). Color scale from blue to red, blue corresponds to vanishing density.

The edge states are visible in the zigzag triangles and hexagons, and they appear as a prominent peak (DOS) at the Fermi energy. For triangles, all the edge states have zero energy, i.e. they are exactly at the Fermi level. The hexagon edge states are also concentrated at the Fermi energy, but they have a small dispersion. The situation is significantly different in round flakes due to the fact that the lengths of the zigzag regions are very small. This leads to a situation where the electrons become localized and their energy increases. Figure 9 shows the total electron density of edge states in these three cases: in the case of triangles, the edge states bend smoothly around the corners of the triangle, but for hexagons they are already pushed out from the corners. The round flakes exhibit edge states that are localized in narrow regions and penetrate much deeper inside the flake.

7. Conclusions

We have computed the electronic structure of triangular, hexagonal and round graphene flakes by using a TB method that considers the carbon p_z electrons. We observe that the DOS close to the Fermi energy ϵ_F is independent of the size of the triangles and armchair-edged hexagons, but depends strongly on the size of the zigzag hexagons and round flakes. The triangles with zigzag edge exhibit the well-known edge states, whereas the armchair triangles show an additional set of 'ghost states' which result from the interplay between the graphene band structure and the plane wave solutions of the wave equation. The same ghost states will emerge in any flake of graphene that can be constructed from equilateral armchair triangles of the same size with additional rows of atoms in the boundaries.

Also hexagons can be constructed with armchair or zigzag edges. In the case of the armchair edge, the shell structure is clear and scalable with the flake size (cf triangles). However, for the zigzag edge the shell structure of the hexagonal confinement is disturbed by the edge states, and the level structure above the Fermi energy depends on the size of the hexagon.

For round graphene dots, one might expect the shell structure of a circular cavity. However, the low-energy level structure (above ϵ_F) is dominated by the edge states that appear in the zigzag regions of the edge, and the lengths and distribution of such segments vary with the flake diameter. Consequently, the level structure is very sensitive to the size of the circular graphene flake.

The effect of the edge roughness on shell structure was studied by removing a fraction of atoms randomly. In the armchair triangles, the shell structure is simple and scalable, and the roughness has only a small effect on the low energy states. For the zigzag hexagons, the low-energy levels are edge-related, and already a small roughness removes the shell structure.

We have obtained our results for free graphene flakes and not considered the interaction with substrate or electric leads which evidently could have effects on the shell structure. However, transport spectroscopy through semiconductor quantum dots [43] has shown that the shell structure calculated for free dots [44] can indeed be captured with weak connections to leads. A more direct measurement of the electronic states would be scanning tunneling microscopy (STM) which has already been used to study suspended graphene [45]. It is possible that on a proper surface, STM spectroscopy could reveal the detailed structures of the electron wave functions.

References

[1] de Heer W A 1993 *Rev. Mod. Phys.* **64** 677
[2] Reimann S M and Manninen M 2002 *Rev. Mod. Phys.* **74** 1283
[3] Mansikka-aho J, Hammarén E and Manninen M 1992 *Phys. Rev.* B **46** 12649
[4] Reimann S M, Koskinen M, Häkkinen H, Lindelof P E and Manninen M 1997 *Phys. Rev.* B **56** 12147
[5] Ekardt W 1984 *Phys. Rev. Lett.* **52** 1925
[6] Manninen M, Mansikka-aho J and Hammarén E 1991 *Europhys. Lett.* **15** 423
[7] Brack M, Blaschke J, Greagh S C, Magner A G, Meier P and Reimann S M 1997 *Z. Phys.* D **40** 276
[8] Kolehmainen J, Häkkinen H and Manninen M 1997 *Z. Phys.* D **40** 306
[9] Janssens E, Tanaka H, Neukermans S, Silverans R E and Lievens P 2003 *New J. Phys.* **5** 46
[10] Reimann S M, Koskinen M, Helgesson J, Lindelof P E and Manninen M 1998 *Phys. Rev.* B **58** 8111
[11] Lai M Y and Wang Y L 1998 *Phys. Rev. Lett.* **81** 164
[12] Berger C *et al* 2004 *J. Phys. Chem.* **108** 19912
[13] Novoselov K S, Geim A K, Morozov S V, Jiang D, Zhang Y, Dubonos S V, Grigorieva I V and Firsov A A 2004 *Science* **306** 666
[14] Novoselov K S, Geim A K, Morozov S V, Jiang D, Katsnelson M I, Grigorieva I V, Dubonos S V and Firsov A A 2005 *Nature* **438** 197
[15] Berger C *et al* 2006 *Science* **312** 1191
[16] Novoselov K S, Jiang Z, Zhang Y, Morozov S V, Stormer H L, Zeitler U, Maan J C, Boebinger G S, Kim P and Geim A K 2007 *Science* **315** 1379
[17] Geim A K and Novoselov K S 2007 *Nat. Mater.* **6** 183
[18] Li G and Andrei E A 2007 *Nat. Phys.* **3** 623
[19] Alicea J and Fisher M P A 2005 *Phys. Rev.* B **74** 75422
[20] Gusynin V P and Sharapov S G 2005 *Phys. Rev. Lett.* **95** 146801
[21] Tworzydlo J, Trauzettel B, Titov M, Rycerz A and Beenakker C W J 2006 *Phys. Rev. Lett.* **96** 246802
[22] Gusynin V P, Sharapov S G and Carbotte J P 2006 *Phys. Rev. Lett.* **96** 256802
[23] Zhou S Y, Gweon G H, Graf J, Fedorov A V, Spataru C D, Diehl R D, Kopelevich Y, Lee D H, Louie S G and Lanzara A 2006 *Nat. Phys.* **2** 595
[24] Yamamoto T, Noguchi T and Watanabe K 2006 *Phys. Rev.* B **74** 121409
[25] Nomura K and MacDonald A H 2007 *Phys. Rev. Lett.* **98** 76602
[26] Son Y W, Cohen M L and Louie S G 2007 *Phys. Rev. Lett.* **97** 216803
[27] Areshkin D A, Gunlycke D and White C T 2007 *Nano Lett.* **7** 204
[28] Chen J-H, Jang C, Xiao S, Ishigami M and Fuhrer M S 2008 *Nat. Nanotechnol.* **3** 206

[29] Castro E V, Peres N M R, Lobes dos Santos J M B, Castro Neto A H and Guinea F 2008 *Phys. Rev. Lett.* **100** 026802
[30] Akhmerov A R and Beenakker C W J 2008 *Phys. Rev.* B **77** 085423
[31] Akola J, Heiskanen H P and Manninen M 2008 *Phys. Rev.* B **77** 193410
[32] Wallace P R 1947 *Phys. Rev.* **71** 622
[33] Elliot S R 1998 *The Physics and Chemistry of Solids* (New York: Wiley)
[34] Son Y-W, Cohen M L and Louie S G 2006 *Nature* **444** 347
[35] Borghis F E and Papas C H 1957 *Encyclopedia of Physics* ed S Flücke (Berlin: Springer)
[36] Lame M G 1852 *Leçons sur le Théorie Mathématique d'Elasticité des Cores Solides* (Paris: Bachelier)
[37] Krishnamurthy H R, Mani H S and Verma H C 1982 *J. Phys. A: Math. Gen.* **15** 2131
[38] Doncheski M A, Hepplemann S, Robinet R W and Tussey D C 2003 *Am. J. Phys.* **71** 541
[39] Castro Neto A H, Guinea F, Peres N M R, Novoselov K S and Geim A K 2008 *Rev. Mod. Phys.* at press (arXiv:0709.1163v2)
[40] Huang Y-Z, Guo W-H, Yu L-J and Lei H-B 2001 *IEEE J. Quantum Electrodyn.* **37** 1259
[41] Kobayashi K 1993 *Phys. Rev.* B **48** 1757
[42] Nakada K, Fujita M, Dresselhaus G and Dresselhaus M S 1996 *Phys. Rev.* B **54** 17954
[43] Tarucha S D, Austing D G, Honda T, van der Haage R J and Kouwenhoven L 1996 *Phys. Rev. Lett.* **77** 3613
[44] Koskinen M, Manninen M and Reimann S M 1997 *Phys. Rev. Lett.* **79** 1389
[45] Li G, Luican A and Andrei E Y 2008 arXiv:0803.4016v1

Eur. Phys. J. D (2009)
DOI: 10.1140/epjd/e2008-00282-0

THE EUROPEAN PHYSICAL JOURNAL D

Regular Article

Electronic shell and supershell structure in graphene flakes

M. Manninen[a], H.P. Heiskanen, and J. Akola

Nanoscience Center, Department of Physics, P.O. Box 35, 40014 University of Jyväskylä, Finland

Received 19 September 2008
Published online 24 January 2009 –

Abstract. We use a simple tight-binding (TB) model to study electronic properties of free graphene flakes. Valence electrons of triangular graphene flakes show a shell and supershell structure which follows an analytical expression derived from the solution of the wave equation for triangular cavity. However, the solution has different selection rules for triangles with armchair and zigzag edges, and roughly 40 000 atoms are needed to see clearly the first supershell oscillation. In the case of spherical flakes, the edge states of the zigzag regions dominate the shell structure which is thus sensitive to the flake diameter and center. A potential well that is made with external gates cannot have true bound states in graphene due to the zero energy band gap. However, it can cause strong resonances in the conduction band.

PACS. 73.21.La Quantum dots – 81.05.Uw Carbon, diamond, graphite – 61.48.De Structure of carbon nanotubes, boron nanotubes, and closely related graphitelike systems – 81.05.Uw Carbon, diamond, graphite

1 Introduction

Electrons confined in a finite cluster of atoms with spherical symmetry exhibit a shell structure [1,2]. In large enough clusters, the shells representing different classical periodic orbits can interfere forming a supershell structure [3,4] that has been observed in large alkali metal clusters [5]. The supershell structure is especially visible in a two-dimensional triangular cavity which has only two classical periodic orbits [6]. The triangular cavity is interesting also due to the fact that the Schrödinger equation and the wave equation are exactly solvable in that system [7–9], and it has been shown that triangular shapes are preferred in two-dimensional nearly free electron systems [10–12].

Recently, experiments have shown that single layer graphene flakes can be prepared on inert surfaces where the graphene-surface interaction is weak [13–18]. Since the manipulation of graphene on different substrates is still a fast developing area, it is not out of question that graphene flakes with accurate shape and size can be eventually processed on a substrate where the interaction is so weak that it does not affect the graphene electronic levels close to the Fermi point. Hence, we study ideal free graphene flakes neglecting the interaction with the substrate. The experiments have inspired a wealth of theoretical studies of graphene [19–32], but according to our knowledge the shell and supershell structure of large graphene flakes has not been addressed except in our recent work [33].

Electronic structure calculations based on the density functional theory (DFT) have shown that the energy levels close to the Fermi level, which consists of discrete points in graphene, are determined by the p electrons perpendicular to the graphene plane (for a review see [34]). A simple tight-binding (TB) model with only one electron per site and only the nearest-neighbour hopping describes well the electronic structure close to the Fermi points as suggested by Wallace already in 1947 [35]. The TB Hamiltonian used is then the simple Hückel model

$$H_{ij} = \begin{cases} -t, \text{ if } \quad i,j \quad \text{nearest} \quad \text{neighbours} \\ 0, \text{ otherwise,} \end{cases} \tag{1}$$

where the hopping parameter t (resonance integral) determines the width of the bands and the on-site energy is chosen to be $\epsilon_F = 0$. We present our results in units $t = 1$ which in real graphene corresponds to ∼2.6 eV. In reality, the flake edges are either passivated (e.g. with hydrogen) or reconstructed in order to remove dangling bonds. The passivation is not expected to affect the perpendicular p-states, and we can simply neglect the existence of such atoms. This has been also validated by our recent DFT calculations [33]. At the bottom of the valence band the TB model results in free-electron-like states with nearly constant density of states (DOS). This allows us to compare these "normal" free-electron states with those of the "massless electrons" at the bottom of the conduction band calculated for the exactly same geometry.

The paper is organized as follows: in Section 2 we discuss the shell and supershell structure in triangular graphene flakes, in Section 3 we show how the edge geometry dominates the shell structure in circular flakes, and in Section 4 we describe quantum dots that have been made with external potentials in an infinite graphene sheet. Section 5 gives the conclusions.

[a] e-mail: Matti.Manninen@phys.jyu.fi

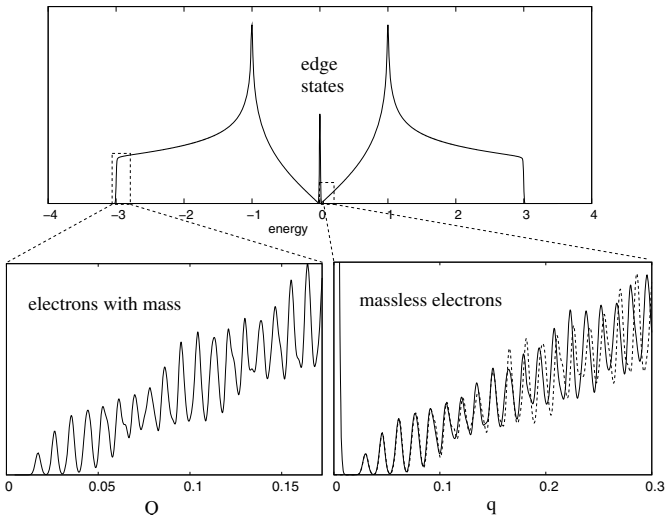

Fig. 1. Upper panel: TB-DOS (p_z electrons) of a graphene triangle with 44 097 atoms and zigzag edges. The discrete energy levels have been smoothened with Gaussians. The peak at zero energy corresponds to the edge states. The lower panels show TB-DOS as a function of the wave number at the bottom of the band (left) and above the Fermi level (right). The dashed line shows the analytical result of equation (3). The wave numbers are: $Q = \sqrt{\epsilon + 3}$ and $q = \epsilon$, where ϵ is the energy in units of $t = 1$. The Gaussian widths have been adjusted in the lower panels in order to show the individual energy levels.

2 Shell structure of triangular graphene flakes

In a triangular cavity with hard walls and a constant potential inside, the two-dimensional Schrödinger equation has an exact solution [8] with energy levels

$$\epsilon_{n,m} = \epsilon_0(n^2 + m^2 - nm), \tag{2}$$

where ϵ_0 depends on the particle mass and the size of the cavity, and m and n are integers with $n \geq 2m \geq 1$. Figure 1 shows the density of states calculated with the TB model (TB-DOS) for a large graphene triangle of 44 097 atoms which has a zigzag edge. In such a large triangle, DOS is similar to that of an infinite graphene sheet except for the appearance of the edge states which appear as a sharp peak at zero energy. A detailed study of the energy levels at the bottom of the valence band reveals that the level structure is nearly exactly described with the analytical formula of equation (2). TB-DOS and equation (2) produce the same curve shown in the lower left corner of the figure. Note that TB-DOS is plotted here as a function of the wave number defined as $Q = \sqrt{\epsilon + 3t}$ (the bottom of the band is $-3t$). The regular oscillation as a function of Q corresponds to the shell structure and the peak amplitude variation (breathing) marks the supershell structure [6]. Triangles with an armchair edge show a similar supershell structure at the bottom of the band [33].

At the bottom of the conduction band, close to $\epsilon = 0$, the dispersion relation of the electron energy is linear, $\epsilon(k) = c\hbar k$, where c is the electron velocity. This means that the electrons behave as massless particles. If we consider the conduction electrons as free particles, we cannot solve the energy eigenvalues from the Schrödinger equation but should use the relativistic Dirac equation [34]. However, we choose here a simpler approach and make an ansatz that the energy eigenvalues are solutions of the Klein-Gordon wave equation with positive energy eigenvalues. This immediately gives

$$\epsilon_{n,m} = \epsilon_1\sqrt{n^2 + m^2 - nm}), \tag{3}$$

which is the same as for normal electrons apart of the square root dependence of the quantum numbers and a different prefactor. The numerical solutions of the TB problem for triangles with a zigzag edge, indeed, show that the energy eigenvalues become more-and-more accurately described with those of equation (3) when the triangle size increases. Figure 1 (lower right panel) compares the result of the ansatz of equation (3) with the full TB calculation for the large triangle. The agreement is nearly perfect up to $\epsilon = 0.1$ (corresponding to 0.25 eV), and the discrepancy at larger energies is due to the increasing nonlinearity and anisotropy of the energy bands.

The results suggests that the supershell structure of the triangular cavity appears in zigzag-edged triangular graphene flakes, but the flake should have at least ca. 40 000 atoms (i.e., $L \geq 40$ nm) before the first supershell oscillation becomes clearly visible. We remark that in the case of armchair edge, equation (3) is still valid, but also indices with $m = n$ are allowed [33]. More detailed results for smaller triangles are described in reference [36], where we also show that the shell structure is quite robust against edge roughness in the close vicinity of the Fermi level.

3 Shell structure in circular graphene flakes

In the case of a two-dimensional cavity with circular symmetry, the energy levels of the Schrödinger equation are determined by the zeroes of the Bessel functions B_j with integer values j. The TB model gives corresponding results at the bottom of the valence band, because the electrons are well represented by nearly free electrons. Following the ideas presented for the triangles one would expect that the energy levels close to the bottom of the conduction band could be determined similarly. However, in this case, the detailed geometry of the edge (perimeter) has a dominant role in determining the energy levels above the Fermi level, and the energy spectrum is very sensitive to the number of atoms in the circular dot, as shown in Figure 2. The circular flakes have been obtained by cutting a circle out of an infinite graphene sheet. Note, that the actual edge geometry depends not only on the radius but also on the site of the center.

The reason for the size-sensitivity can be traced back to the edge states which are present in graphene constructions with zigzag edges. In circular dots, the perimeter has short regions of zigzag segments that are mixed with other motifs (especially armchair). This roughness causes edge states with different energies, which is in sharp contrast to the zigzag triangles where all the edge

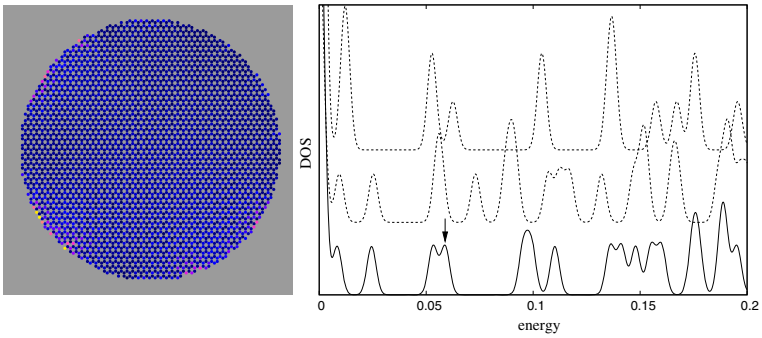

Fig. 2. (Color online) Geometry of a circular dot cut out from a graphene sheet (left) showing electrons density of the state indicated with an arrow (black is zero density, yellow high density). The three curves (right) show TB-DOS just above the Fermi energy for three circular flakes with different positions of the circle's centre and with 3868 (bottom curve), 3864 (middle curve), and 3868 atoms (top curve), respectively, demonstrating the sensitivity of the level structure on edge geometry.

states have exactly zero energy in the TB model. Figure 2 shows the electron density of one such state with density maximas at the surface.

Usually, the shell structure is determined by the overall shape of the confining potential in metallic and semiconductor quantum dots, and the detailed atomic structure does not play any role due to the fact that the electron wave length is much larger than the interatomic spacing. This is not the case in the circular graphene flakes. Although the wavelength of the "Dirac electron" is still much larger than the interatomic spacing, the tendency for localization of electrons close to the zigzag edges destroys the simple shell structure, and different circular flakes result in qualitatively different electron levels as shown in Figure 2.

4 Quantum dots prepared with external potential

So far, we have studied free graphene flakes where the electron confinement is determined by the flake edges. In semiconductor heterostructures, quantum dots are usually prepared by confining the delocalized conduction electrons in a small region with external gates (for a review see [37]). It is expected that a similar technique can be applied in the future also for the two-dimensional gas of "Dirac electrons" in graphene. External gates form nearly harmonic confinement close to the center of the quantum dot. Another possibility for supported graphene flakes could be to modify the atomic structure of the substrate so that different regions would comprise different elements, and, consequently, cause different interaction with the adsorbate. In this case, the resulting potential well could be more of the square-well-type than harmonic.

The situation is different for an external confinement (infinite graphene sheet) than for a finite flake with edges. Since there is no band gap in graphene, an external potential well cannot bind an electron as demonstrated in Figure 3. In addition, this differs considerably from the quantum dots manufactured from semiconductor heterostructures, where bound electronic states can exist inside the band gap of the semiconductor in question.

We have studied the effect of an external confinement by using a large hexagonal graphene flake with 4902 atoms. An external potential was added at the center

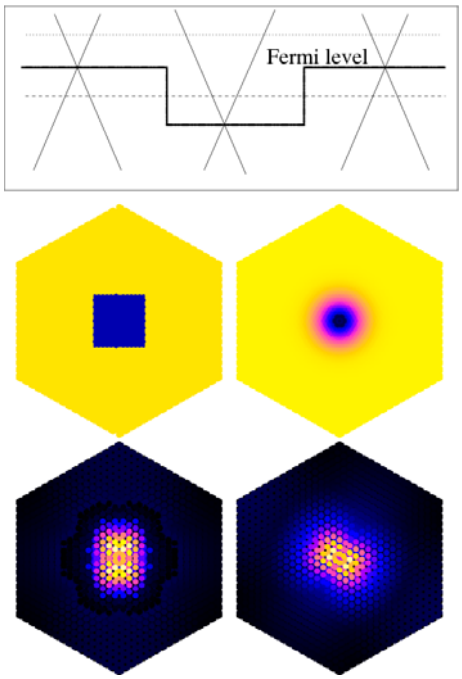

Fig. 3. (Color online) The upper panel shows an external square well potential in graphene and schematically the linear energy bands in different regions. Electrons cannot be localized by the potential, because a conduction electron inside the well (dashed line) can move out as a valence electron. The two figures in the middle display a square-shaped and circular Gaussian potential wells in a hexagonal graphene flake. The lower two figures illustrate the electron densities of a resonance state above the Fermi level (dotted line in the upper panel).

of the flake. We considered three different external potentials: a circular well, a square-shaped well, and a smooth Gaussian potential with circular symmetry. Surprisingly, the results are qualitatively similar irrespective of the type of the attractive potential. Bound states appear at the bottom of the valence band where the electrons act as normal free electrons. In the more interesting region close to the Fermi level, no bound states can be observed. However, above the Fermi level all the potentials result in strong resonances with a large enhancement of the wave function amplitude within the potential well region. Figure 3 shows the densities of the wave functions for two such resonances. The wave functions do not decay to zero outside the potential well but reach a small and uniform amplitude that

goes all the way to the flake edge (the small amplitude is not visible Fig. 3).

For a potential barrier, the penetration of a wave function inside an apparently forbidden region is often referred to as the Klein paradox [34], which has its origin in the Dirac theory of massless fermions. As Figure 3 shows for the TB (band structure) model, the wave function penetration inside the "forbidden region" is a natural consequence of the missing band gap: an electron that appears on the conduction band on one side of the step continues as a valence electron on the other side.

5 Conclusions

We have studied the possibility of observing electronic shell and supershell structure in free graphene flakes. For this purpose, we have used a simple tight-binding model with one electron per atomic site (p_z electrons). Despite its simplicity, the TB model describes the key features of the graphene band structure close to the Fermi points.

In large triangular flakes with zigzag edges, the shell structure of the "Dirac electrons" in the conduction band is the same as for free electrons in a triangular cavity. The analytical expression gives the energy levels accurately up to $\sim$0.25 eV above the Fermi energy, and the number of shells within this region depends on the number of atoms in the triangle. A triangle of ca. 40 000 atoms ($L \geq 40$ nm) shows already the first supershell oscillation.

In the case of circular graphene flakes, the shell structure above the Fermi level is dominated by the states that are localized close to the zigzag regions of the edges. This makes the shell structure very sensitive, not only to the radius of the circular flake (number of atoms) but also to the location of the center.

Potential wells which are created on an infinite graphene sheet with external potentials (e.g. external gates, inhomogeneous substrate) cannot localize electrons. This is a consequence of the missing band gap in the graphene band structure. However, such potential wells cause resonance states above the Fermi level, which can strongly affect the conductance of narrow graphene strips.

This work has been supported by the Academy of Finland.

References

1. J.L. Martins, R. Car, J. Buttet, Surf. Sci. **106**, 265 (1981)
2. W.A. De Heer WA, Rev. Mod. Phys. **64**, 677 (1993)
3. R. Balian, C. Bloch, Ann. Phys. **60**, 401 (1970)
4. H. Nishioka, K. Hansen, B. Mottelson, Phys. Rev. B **42**, 9377 (1990)
5. J. Pedersen, S. Bjørnholm, J. Borgreen, K. Hansen, T.P. Martin, H.D. Rasmunssen, Nature **353**, 733 (1991)
6. M. Brack, J. Blaschke, S.C. Greagh, A.G. Magner, P. Meier, S.M. Reimann, Z. Phys. D **40**, 276 (1997)
7. M.G. Lame, *Leçons sur la Théorie Mathématique d'Élasticité des Corps Solides* (Bachelier, Paris, 1852)
8. H.R. Krishnamurthy, H.S. Mani, H.C. Verma, J. Phys. A: Math. Gen. **15**, 2131 (1982)
9. M.A. Doncheski, S. Hepplemann, R.W. Robinet, D.C. Tussey, Am. J. Phys. **71**, 541 (2003)
10. S.M. Reimann, M. Koskinen, H. Häkkinen, P.E. Lindelof, M. Manninen, Phys. Rev. B **56**, 12147 (1997)
11. J. Kolehmainen, H. Häkkinen, M. Manninen, Z. Phys. D **40**, 306 (1997)
12. S.M. Reimann, M. Koskinen, J. Helgesson, P.E. Lindelof, M. Manninen, Phys. Rev. B **58**, 8111 (1998)
13. C. Berger, Z.M. Song, T.B. Li, X.B. Li, A.Y. Ogbazghi, R. Feng, Z.T. Dai, A.N. Marchenkov, E.H. Conrad, P.N. First, W.A. De Heer, J. Phys. Chem. **108**, 19912 (2004)
14. K.S. Novoselov, A.K. Geim, S.V. Morozov, D. Jiang, Y. Zhang, S.V. Dubonos, I.V. Grigorieva, A.A. Firsov, Science **306**, 666 (2004)
15. C. Berger, Z.M. Song, X.B. Li, X.S. Wu, N. Brown, C. Naud, D. Mayo, T.B. Li, J. Hass, A.N. Marchenkov, E.H. Conrad, P.N. First, W.A. De Heer, Science **312**, 1191 (2007)
16. K.S. Novoselov, Z. Jiang, Y. Zhang, S.V. Morozov, H.L. Stormer, U. Zeitler, J.C. Maan, G.S. Boebinger, P. Kim, A.K. Geim, Science **315**, 1379 (2007)
17. A.K. Geim, K.S. Novoselov, Nature Mater. **6**, 183 (2007)
18. G. Li, E.A. Andrei, Nature Phys. **3**, 623 (2007)
19. J. Alicea, M.P.A. Fisher, Phys. Rev. B **74**, 75422 (2005)
20. V.P. Gusynin, S.G. Sharapov, Phys. Rev. Lett. **95**, 146801 (2005)
21. J. Tworzydlo, B. Trauzettel, M. Titov, A. Rycerz, C.W.J. Beenakker, Phys. Rev. Lett. **96**, 246802 (2006)
22. V.P. Gusynin, S.G. Sharapov, J.P. Carbotte, Phys. Rev. Lett. **96**, 256802 (2006)
23. S.Y. Zhou, G.H. Gweon, J. Graf, A.V. Fedorov, C.D. Spataru, R.D. Diehl, Y. Kopelevich, D.H. Lee, S.G. Louie, A. Lanzara, Nature Phys. **2**, 595 (2006)
24. T. Yamamoto, T. Noguchi, K. Watanabe, Phys. Rev. B **74**, 121409 (2006)
25. K. Nomura, A.H. MacDonald, Phys. Rev. Lett. **98**, 76602 (2007)
26. Y.W. Son, M.L. Cohen, S.G. Louie, Phys. Rev. Lett. **97**, 216803 (2007)
27. D.A. Areshkin, D. Gunlycke, C.T. White, Nano Lett. **7**, 204 (2007)
28. J. Fernández-Rossier, J.J. Palacios, Phys. Rev. Lett. **99**, 177204 (2007)
29. J.-H. Chen, C. Jang, S. Xiao, M. Ishigami, M.S. Fuhrer, Nature Nanotech. **3**, 206 (2008)
30. E.V. Castro, N.M.R. Peres, J.M.B. Lobes dos Santos, A.H. Castro Neto, F. Guinea, Phys. Rev. Lett. **100**, 026802 (2008)
31. A.R. Akhmerov, C.W.J. Beenakker, Phys. Rev. B **77**, 085423 (2008)
32. Z.Z. Zhang, K. Chang, F.M. Peeters, Phys. Rev. B **77**, 235411 (2008)
33. J. Akola, H.P. Heiskanen, M. Manninen, Phys. Rev. B **77**, 193410 (2008)
34. A.H. Castro Neto, F. Guinea, N.M.R. Peres, K.S. Novoselov, A.K. Geim, e-print `arXiv:0709.1163v2`
35. P.R. Wallace, Phys. Rev. **71**, 622 (1947)
36. H.P. Heiskanen, J. Akola, M. Manninen, New J. Phys. **10**, 103015 (2008)
37. S.M. Reimann, M. Manninen, Rev. Mod. Phys. **74**, 1283 (2002)